

# Optimal Scheme for Quantum Metrology

Jing Liu,<sup>1,\*</sup> Mao Zhang,<sup>1</sup> Hongzhen Chen,<sup>2</sup> Lingna Wang,<sup>2</sup> and Haidong Yuan<sup>2,†</sup>

<sup>1</sup>*MOE Key Laboratory of Fundamental Physical Quantities Measurement, PGMF and School of Physics, Huazhong University of Science and Technology, Wuhan 430074, China*

<sup>2</sup>*Department of Mechanical and Automation Engineering, The Chinese University of Hong Kong, Shatin, Hong Kong*

Quantum metrology can achieve far better precision than classical metrology, and is one of the most important applications of quantum technologies in the real world. To attain the highest precision promised by quantum metrology, all steps of the schemes need to be optimized, which include the state preparation, parameterization and measurement. Here we review the recent progresses on the optimization of these steps, which are essential for the identification and achievement of the ultimate precision limit in quantum metrology. We hope this provides a useful reference for the researchers in quantum metrology and related fields.

## I. INTRODUCTION

Metrology, which studies the precision limit of measurement and estimation, plays a central role in science and technology. Recently quantum metrology, which exploits quantum mechanical effects to achieve far better precision than classical schemes [1–22], has gained increasing attention and has found wide applications in various fields, such as gravitational wavedetection [19, 23–27], quantum phase estimation [5, 28–31], quantum magnetometer [32, 33], quantum ranging [34–36], quantum spectroscopy [37–40], quantum imaging [41–47], quantum target-detection [48, 49], quantum gyroscope [50, 51], distributed quantum sensing [52–54], atomic clocksynchronization [55–61], and even biological measurements [62].

A central task in quantum metrology is to identify the ultimate precision limit that can be achieved with given resources and design schemes to attain it. In the finite regime where the number of the measurement is limited, this is usually a hard task. When one does not have sufficient prior information of the parameter, this is a ‘global’ problem in the sense that the chosen cost function need to be minimized over a certain region. This is often handled by minimizing the mean of the cost function or minimizing the worst case over the region [63–65] for which the optimal scheme is only known for very symmetric cases [66–70]. The task is much simpler when the number of the measurement can be asymptotically large, in this case the value of the parameter can be pinpointed asymptotically and the ‘global’ problem becomes ‘local’. In this regime, a well-behaved cost function can be approximated by the variance, which corresponds to the second order expansion of the cost function around the true value, and the local precision limit can be quantified by the quantum Cramér-Rao bound [1, 2]. The studies on the optimal schemes for the single-parameter estimation in the asymptotic limit have made much progress recently, which will be the focus of this review. For the

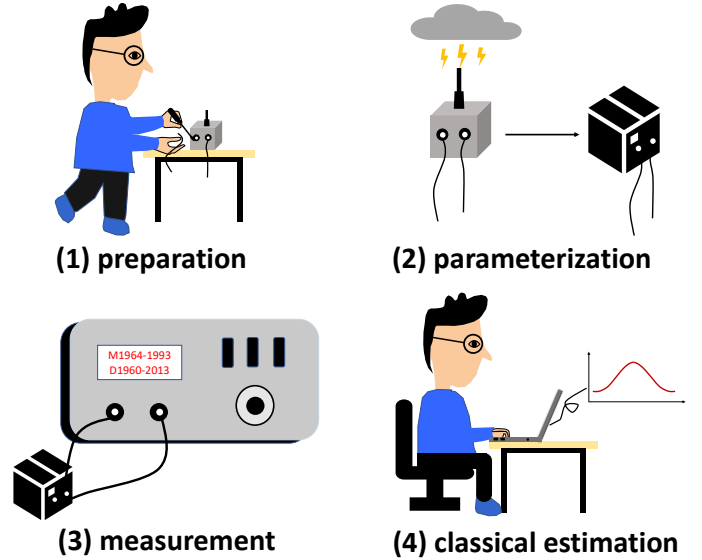


FIG. 1. The schematic for a general process of quantum parameter estimation, which includes four steps: (1) preparation; (2) parameterization; (3) measurement; and (4) classical estimation. The first three steps (“ppm” steps) are the major subjects in quantum metrology.

progresses on the multi-parameter estimation, we refer the readers to the recent reviews [39, 71–73].

A general protocol of quantum metrology typically consists of four steps: (1) preparation; (2) parameterization; (3) measurement and (4) estimation, as illustrated in Fig. 1. To achieve the best precision, all steps need to be optimized. The optimization of the last step is a well-studied subject in the classical statistics, in this review, we will focus on the optimization of the first three steps (quantum part), denoted as “ppm”<sup>1</sup>. Interestingly, “ppm” is also one of the most well-used pseudo-units in the field of precision measurements, standing for one part per million. In Sec. II we first review the quantum dy-

\* liujingphys@hust.edu.cn

† hdyuan@mae.cuhk.edu.hk

<sup>1</sup> The initials of preparation, parameterization and measurement.

namics and the quantum Cramér-Rao bound, which are the main tools used to quantify the precision limit of the single-parameter quantum estimation. Section III to V focus on the current development on the optimizations of the first three steps. Specifically, in Sec. III we review the progresses on the optimization of the initial probe states. In Sec. IV, we review the progresses on the optimization of the parametrization, which we mainly focus on the quantum control and quantum error correction. In Sec. V we review the optimization of the measurement, mainly on the local adaptive measurements, which is practically easier to implement. We make a summary in Sec. VI.

## II. QUANTUM DYNAMICS AND METROLOGICAL BOUNDS

### A. Quantum dynamics

Quantum dynamics is the foundation of quantum information, and even quantum mechanics. For an isolated quantum system, the dynamics is depicted by the Schrödinger equation  $\partial_t|\psi\rangle = -iH|\psi\rangle$  for quantum state  $|\psi\rangle$  or Liouville equation  $\partial_t\rho = -i[H, \rho]$  for density matrix  $\rho$ . Here  $H$  is the Hamiltonian. The solution for this equation is  $\rho(t) = U(t)\rho_{\text{in}}U^\dagger(t)$  with  $U(t) = \mathcal{T}\exp(-i\int_0^t H(\tau)d\tau)$  a unitary operator.  $\mathcal{T}$  is the time-ordering operator. It reduces to  $\exp(-iHt)$  if  $H$  is time-independent. Once the quantum noise is involved, the evolution is not unitary any more. Two typical approaches to depict the noisy dynamics are the integral and differential methods. The most widely used integral method is the Kraus representation, which can model general completely positive and trace-preserving maps, and thereby a routine analytical representation for the integrated quantum dynamics, which acts as quantum channels on the probe states. In this representation, the output state of a quantum channel  $\mathcal{E}(\cdot)$ , with the initial probe state as  $\rho_{\text{in}}$ , can be described as

$$\mathcal{E}(\rho_{\text{in}}) = \sum_{j=1}^m K_j \rho_{\text{in}} K_j^\dagger, \quad (1)$$

where  $K_j$  is a Kraus operator satisfying  $\sum_j K_j^\dagger K_j = \mathbb{1}$  with  $\mathbb{1}$  the identity operator. Note that given a quantum channel, the associated Kraus operators are not unique. Any isometry, which satisfies  $V^\dagger V = \mathbb{1}_m$  with  $V \in \mathbb{C}^{p \times m}$  ( $p \geq m$ ), can lead to an equivalent set of Kraus operators as  $\tilde{K}_j = \sum_i v_{ji} K_i$  with  $v_{ji}$  the  $j$ th entry of  $V$ . Such equivalent Kraus operators can be obtained by first appending  $p-m$  zero operators as  $\{K_1, \dots, K_m, \mathbf{0}, \dots, \mathbf{0}\}$ , then making an equivalent unitary transformation on these expanded operators,  $\tilde{K}_j = \sum_i v_{ji} K_i$ , here  $v_{ji}$  are the entries of the first  $m$  columns of a  $p \times p$  unitary matrix (the entries of the remaining  $p-m$  columns do not appear as they act on the zero operators).

The dynamics can also be described with the differential equations. A widely used form that describes the Markovian dynamics is the master equation

$$\partial_t \rho = -i[H, \rho] + \sum_k \left( \Gamma_k \rho \Gamma_k^\dagger - \frac{1}{2} \{ \Gamma_k^\dagger \Gamma_k, \rho \} \right), \quad (2)$$

where  $\Gamma_k$  is the  $k$ th Lindblad operator.

### B. Quantum Cramér-Rao bounds

To estimate the value of a parameter,  $x_{\text{true}}$ , from certain amount of data that is sampled from a conditional probability distribution that depends on the parameter—we use  $p(y|x)$  to denote the conditional probability of event  $y$  given  $x$ , the Cramér-Rao bound provides an asymptotically achievable lower bound on the variance of any locally unbiased estimators as [74, 75]

$$\text{var}(\hat{x}) \geq \frac{1}{nI_x}, \quad (3)$$

here  $\hat{x}$  is a locally unbiased estimator which satisfies  $E(\hat{x}) = x_{\text{true}}$ ,  $\frac{d}{dx}E(\hat{x})|_{x_{\text{true}}} = 1$ ,  $\text{var}(\hat{x}) = E[(\hat{x} - E(\hat{x}))^2]$  is the variance of the estimator,  $n$  is the number of sampled data and

$$I_x = \int_y \frac{[\partial_x p(y|x)]^2}{p(y|x)} dy \quad (4)$$

is the Fisher information [76]. For multiple unknown parameters

$$\mathbf{x} = (x_0, x_1, \dots, x_m, \dots)^T, \quad (5)$$

the counterpart of the variance is the covariance matrix  $\text{cov}(\hat{\mathbf{x}})$ , where the  $jk$ -th entry is given by

$$[\text{cov}(\hat{\mathbf{x}})]_{jk} = \int_y p(y|x) [\hat{x}_j - E(\hat{x}_j)] [\hat{x}_k - E(\hat{x}_k)] dy \quad (6)$$

with  $\hat{x}_{j(k)}$  as the locally unbiased estimator for  $x_{j(k)}$ . It is easy to see that the diagonal entries of the covariance matrix are just the variances for the corresponding parameters. The multi-parameter Cramér-Rao bound is given by

$$\text{cov}(\hat{\mathbf{x}}) \geq \frac{1}{n} I_{\mathbf{x}}^{-1}, \quad (7)$$

where  $I_{\mathbf{x}}$  is now the Fisher information matrix with the  $jk$ -th entry given by

$$(I_{\mathbf{x}})_{jk} = \int_y \frac{\partial_{x_j} p(y|x) \partial_{x_k} p(y|x)}{p(y|x)} dy. \quad (8)$$

The Cramér-Rao bound can be achieved asymptotically when  $n \rightarrow \infty$ .

In quantum parameter estimation, the data is obtained from the measurements on the quantum state,

$\rho(x)$ , which depends on the unknown parameter. The most general measurement in quantum mechanics is the positive operator-valued measure (POVM), which can be described by a set of positive semidefinite operators,  $\{\Pi_i\}$ , that satisfies  $\sum_i \Pi_i = \mathbf{I}$ . The probability of the measurement result,  $p(i|x)$ , which for simplicity we also denote as  $p_i(x)$ , can be obtained as  $p_i(x) = \text{Tr}[\rho(x)\Pi_i]$ . From which we can get the Fisher information

$$I_x = \sum_i \frac{[\partial_x p_i(x)]^2}{p_i(x)}. \quad (9)$$

The quantum Fisher information (QFI) [1, 2], denoted as  $F_x$ , corresponds to the maximal of the Fisher information over all POVMs,

$$F_x = \max_{\{\Pi_i\}} I_x(\{\Pi_i\}). \quad (10)$$

This leads to the quantum Cramér-Rao bound as

$$\text{var}(\hat{x}) \geq \frac{1}{nF_x}, \quad (11)$$

which is asymptotically achievable in the case of the single-parameter estimation.

For multiple parameters, the quantum Cramér-Rao bound is given by

$$\text{cov}(\hat{\mathbf{x}}) \geq \frac{1}{n} \mathcal{F}^{-1}, \quad (12)$$

where  $\mathcal{F}$  is now the quantum Fisher information matrix (QFIM). The entries of the QFIM can be obtained as

$$\mathcal{F}_{jk} = \frac{1}{2} \text{Tr}(\rho \{L_j, L_k\}), \quad (13)$$

where  $L_j$  is the symmetric logarithmic derivative (SLD) corresponding to the parameter  $x_j$ , which is the solution to the equation  $\partial_{x_j} \rho = \frac{1}{2}(\rho L_j + L_j \rho)$ ,  $\{L_j, L_k\} = L_j L_k + L_k L_j$  is the anti-commutator. In the case of the single-parameter estimation, the QFIM reduces to the QFI, which is a scalar given by

$$F_x = \text{Tr}(\rho L_x^2) \quad (14)$$

where  $L_x$  is the SLD for the single parameter  $x$ . For single-parameter estimation, the quantum Cramér-Rao bound can be saturated by the projective measurement on the eigenvectors of the SLD and the maximum likelihood estimations [1–3], while the multi-parameter quantum Cramér-Rao bound is in general not attainable due to the incompatibility of the optimal measurements for different parameters.

The quantum Fisher information is closely related to the geometry of the quantum states. In particular, it is closely related to the fidelity, an important concept for the distinguishment of two quantum states. A widely used form of the fidelity between two quantum states,

$\rho_1$  and  $\rho_2$ , is  $f(\rho_1, \rho_2) := \text{Tr} \sqrt{\sqrt{\rho_1} \rho_2 \sqrt{\rho_1}}$  [77, 78]. This leads to a distance measure on quantum states as

$$D(\rho_1, \rho_2) := \sqrt{2 - 2f(\rho_1, \rho_2)}, \quad (15)$$

which is referred to as the Bures distance. The fidelity can also be used to define the Bures angle as  $\Theta(\rho_1, \rho_2) = \arccos f(\rho_1, \rho_2)$ , which is also a valid metric on the state space. The QFI is proportional to the second order expansion of the Bures distance [6], i.e., up to the second order of  $dx$

$$D(\rho_x, \rho_{x+dx}) = \frac{1}{4} F_x(\rho_x) dx^2, \quad (16)$$

which shows that the QFI is nothing but the fidelity susceptibility (ignoring the constant). A rigorous proof of this relation for arbitrary-rank density matrices can be found in Refs. [39, 79] when the support is fixed.

The connection between the fidelity and the Fisher information can be generalized to quantum channels [80]. Specifically given two quantum channels (the number of the Kraus operators for both channels, denoted as  $m$ , are assumed to be the same as we can always append zero operators if they are not the same initially),

$$\begin{aligned} \mathcal{E}_1(\rho) &= \sum_{i=1}^m K_{1,i} \rho K_{1,i}^\dagger, \\ \mathcal{E}_2(\rho) &= \sum_{i=1}^m K_{2,i} \rho K_{2,i}^\dagger, \end{aligned} \quad (17)$$

the fidelity between two channels is given by [80]

$$f_{\text{qc}}(\mathcal{E}_1, \mathcal{E}_2) = \max_{\|W\|_{\text{op}} \leq 1} \frac{1}{2} \lambda_{\min}(\mathcal{K} + \mathcal{K}^\dagger), \quad (18)$$

where  $\lambda_{\min}(\mathcal{K} + \mathcal{K}^\dagger)$  denotes the minimum eigenvalue of  $\mathcal{K} + \mathcal{K}^\dagger$  with  $\mathcal{K} = \sum_{ij} w_{ij} K_{1,i}^\dagger K_{2,j}$ ,  $w_{ij}$  is the  $ij$ th entry of any matrix,  $W$ , that satisfies  $\|W\|_{\text{op}} \leq 1$  with  $\|\cdot\|_{\text{op}}$  denoting the operator norm which equals to the largest singular value. Here  $W$  comes from the non-uniqueness of the Kraus representation for a quantum channel. Basically, given the equivalent Kraus operators,  $\tilde{K}_{1,q} = \sum_i [V_1]_{qi} K_{1,i}$  and  $\tilde{K}_{2,q} = \sum_i [V_2]_{qi} K_{2,i}$ , with  $V_1, V_2 \in \mathbb{C}^{p \times m}$  as isometries, we have  $\sum_q \tilde{K}_{1,q}^\dagger \tilde{K}_{2,q} = \sum_{ij} w_{ij} K_{1,i}^\dagger K_{2,j}$  where  $w_{ij}$  are entries of  $W = V_1^\dagger V_2$  with  $\|W\|_{\text{op}} \leq \|V_1^\dagger\|_{\text{op}} \|V_2\|_{\text{op}} = 1$ , i.e.,

$$\begin{aligned} & \max_{\|W\|_{\text{op}} \leq 1} \frac{1}{2} \lambda_{\min}(\mathcal{K} + \mathcal{K}^\dagger) \\ &= \max_{\{\tilde{K}_{1,q}\}, \{\tilde{K}_{2,q}\}} \frac{1}{2} \lambda_{\min} \left( \sum_q \tilde{K}_{1,q}^\dagger \tilde{K}_{2,q} + \tilde{K}_{2,q}^\dagger \tilde{K}_{1,q} \right). \end{aligned}$$

The fidelity on quantum channels can be efficiently computed through the semidefinite programming as

$$\begin{aligned} f_{\text{qc}} &= \max \frac{1}{2} y, \\ \text{s.t. } & \begin{cases} \begin{pmatrix} \mathbf{1} & W^\dagger \\ W & \mathbf{I} \end{pmatrix} \geq 0, \\ \mathcal{K} + \mathcal{K}^\dagger - y\mathbf{I} \geq 0. \end{cases} \end{aligned} \quad (19)$$

Similar as the Bures distance on quantum states, we can define the Bures distance on quantum channels as

$$D_{\text{qc}}(\mathcal{E}_1, \mathcal{E}_2) = \sqrt{2 - 2f_{\text{qc}}(\mathcal{E}_1, \mathcal{E}_2)}. \quad (20)$$

The Bures distance on quantum channels corresponds to the minimal operator distance among the equivalent Kraus operators of the quantum channels as

$$\begin{aligned} & \min_{\{\tilde{K}_{1,q}\}, \{\tilde{K}_{2,q}\}} \left\| \sum_q (\tilde{K}_{1,q} - \tilde{K}_{2,q})^\dagger (\tilde{K}_{1,q} - \tilde{K}_{2,q}) \right\|_{\text{op}} \\ &= 2 - \max_{\{\tilde{K}_{1,q}\}, \{\tilde{K}_{2,q}\}} \lambda_{\min} \left( \sum_q \tilde{K}_{1,q}^\dagger \tilde{K}_{2,q} + \tilde{K}_{2,q}^\dagger \tilde{K}_{1,q} \right) \\ &= 2 - 2f_{\text{qc}}(\mathcal{E}_1, \mathcal{E}_2). \end{aligned} \quad (21)$$

The quantum channels can be equivalently represented as  $\mathcal{E}_i(\rho_S) = \text{Tr}_E(U_{\text{ES},i}(|0_E\rangle\langle 0_E| \otimes \rho_S)U_{\text{ES},i}^\dagger)$ , where  $|0_E\rangle$  denotes some standard state of the environment, and  $U_{\text{ES},i}$  is a unitary operator acting on both the system and environment, which is called the unitary extension of  $\mathcal{E}_i$ . Similar to the Uhlmann's purification on quantum states [81], the fidelity function on quantum channels also satisfies

$$f_{\text{qc}}(\mathcal{E}_1, \mathcal{E}_2) = \max_{U_{\text{ES},1}} f_{\text{qc}}(U_{\text{ES},1}, U_{\text{ES},2}) \quad (22)$$

$$= \max_{U_{\text{ES},2}} f_{\text{qc}}(U_{\text{ES},1}, U_{\text{ES},2}). \quad (23)$$

Operationally the fidelity between quantum channels equals to the minimal fidelity between the output states of the extended channels as [80, 82, 83]

$$f_{\text{qc}}(\mathcal{E}_1, \mathcal{E}_2) = \min_{\rho_{\text{SA}}} f[\mathcal{E}_1 \otimes \mathbf{I}(\rho_{\text{SA}}), \mathcal{E}_2 \otimes \mathbf{I}(\rho_{\text{SA}})], \quad (24)$$

where  $\rho_{\text{SA}}$  denotes a state on the system+ancilla, and  $\mathbf{I}$  is the identity operator on the ancillary system. This can be seen as an extension of the operational meaning of the fidelity between quantum states, which equals to the minimal classical fidelity between the probability distributions of the measurement result as

$$f(\rho_1, \rho_2) = \min_{\{E_i\}} f_{\text{cl}}(p_1, p_2), \quad (25)$$

where  $f_{\text{cl}}(p_1, p_2) = \sum_i \sqrt{p_{1,i} p_{2,i}}$  is the classical fidelity with  $p_{1,i} = \text{Tr}(\rho_1 \Pi_i)$  and  $p_{2,i} = \text{Tr}(\rho_2 \Pi_i)$ . It is also known as Bhattacharyya coefficient [84].

The Bures angle can also be extended to the quantum channels as

$$\Theta_{\text{qc}}(\mathcal{E}_1, \mathcal{E}_2) = \arccos f_{\text{qc}}(\mathcal{E}_1, \mathcal{E}_2). \quad (26)$$

The corresponding quantum channel Fisher information, which is the maximal quantum Fisher information over all input states of the extended channel  $\mathcal{E}_x \otimes \mathbf{I}$ , can be related to the Bures angle as

$$F_{\text{qc},x} = \lim_{\delta x \rightarrow 0} \frac{4\Theta_{\text{qc}}^2(\mathcal{E}_x, \mathcal{E}_{x+\delta x})}{\delta x^2}. \quad (27)$$

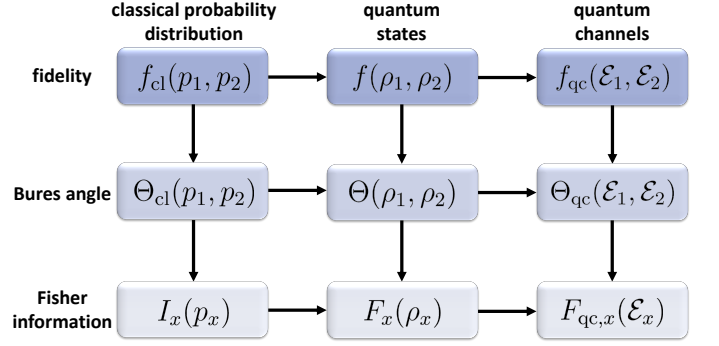


FIG. 2. A unified framework for the discriminations of classical probability distributions, quantum states and quantum channels, here  $f_{\text{cl}}(p_1, p_2) = \sum_i \sqrt{p_{1,i} p_{2,i}}$  with  $p_{1,i} = \text{Tr}(\rho_1 \Pi_i)$  and  $p_{2,i} = \text{Tr}(\rho_2 \Pi_i)$ ,  $f(\rho_1, \rho_2) = \text{Tr}(\sqrt{\rho_1^{\frac{1}{2}} \rho_2 \rho_1^{\frac{1}{2}}})$ , and  $f_{\text{qc}} = \max_{\|W\|_{\text{op}} \leq 1} \frac{1}{2} \lambda_{\min}(\mathcal{K} + \mathcal{K}^\dagger)$  as given in Eq. (18),  $\Theta_{\text{cl}} = \arccos f_{\text{cl}}$ ,  $\Theta = \arccos f$ ,  $\Theta_{\text{qc}} = \arccos f_{\text{qc}}$ , and the corresponding Fisher information  $I_x$ ,  $F_x$  and  $F_{\text{qc},x}$  are given in Eqs. (28), (29) and (27), respectively. The quantities associated with the quantum states equal to the optimal value of the corresponding quantities on the classical probability distribution after the optimization of the measurement, and the quantities on quantum channels equal to the optimal value of the corresponding quantities on quantum states after the optimization of the initial probe states.

We then have a hierarchy of the Fisher information as

$$I_x(p_x) = \lim_{\delta x \rightarrow 0} \frac{4\Theta_{\text{cl}}^2(p_x, p_{x+\delta x})}{\delta x^2}, \quad (28)$$

$$F_x(\rho_x) = \lim_{\delta x \rightarrow 0} \frac{4\Theta^2(\rho_x, \rho_{x+\delta x})}{\delta x^2}, \quad (29)$$

$$F_{\text{qc},x}(\mathcal{E}_x) = \lim_{\delta x \rightarrow 0} \frac{4\Theta_{\text{qc}}^2(\mathcal{E}_x, \mathcal{E}_{x+\delta x})}{\delta x^2}. \quad (30)$$

where  $\Theta_{\text{cl}}(p_x, p_{x+\delta x}) = \arccos f_{\text{cl}}(p_x, p_{x+\delta x})$  can be interpreted as the Bures angle between classical probabilities and  $\Theta(\rho_x, \rho_{x+\delta x}) = \arccos f(\rho_x, \rho_{x+\delta x})$  is the Bures angle between quantum states. This is summarized in Fig. 2, in which the quantities on quantum states equal to the corresponding quantities on the probability distribution over the optimization of the measurement and the quantities on the quantum channels equal to the corresponding quantities on quantum states over the optimization of the input states.

This is based on the purification approach developed in [8, 9, 11, 12, 85, 86], which focus on the neighboring channels that are relevant to the local precision limit. Given a quantum channel  $\mathcal{E}_x(\rho) = \sum_i K_i(x) \rho K_i^\dagger(x)$ , the QFI, in terms of the initial probe state and the Kraus operators, can be written as

$$F_x = \min_{\{\tilde{K}_j\}} C_F(\rho_{\text{in}}, \{\tilde{K}_j\}), \quad (31)$$

where  $C_F = 4(\langle G_1 \rangle_{\text{in}} - \langle G_2 \rangle_{\text{in}}^2)$ ,  $\rho_{\text{in}}$  is the input probe state of the system (or the system+ancilla) and

$\langle G_{1(2)} \rangle_{\text{in}} := \text{Tr}(G_{1(2)} \rho_{\text{in}})$  with

$$G_1 = \sum_j (\partial_x \tilde{K}_j^\dagger)(\partial_x \tilde{K}_j), \quad G_2 = i \sum_j (\partial_x \tilde{K}_j^\dagger) \tilde{K}_j. \quad (32)$$

Here  $\{\tilde{K}_j\}$  is a set of equivalent Kraus operators of the channel. The channel Fisher information, after optimizing  $\rho_{\text{in}}$  on the system+ancilla, is given by

$$F_{\text{qc},x} = \max_{\{\tilde{K}_j\}} \|G_1\|_{\text{op}}. \quad (33)$$

This expression of the channel QFI is equivalent to the channel QFI in Eq. (27) [83]. By restricting the equivalent transformation of the Kraus operators to unitary transformation, i.e.,  $\tilde{K}_j = \sum_p v_{jp} K_p$  with  $V$  (with the  $jp$ -th entry as  $v_{jp}$ ) as unitary instead of isometry, alternative semi-definite programming that computes the channel QFI in Eq. (33) has also been developed [12, 86]. If the channel is used  $N$  times, it can be shown that for any input state, the QFI is upper bounded by [8, 9, 11, 12, 86]

$$4 \min_{\{\tilde{K}_j\}} [N \|G_1\|_{\text{op}} + N(N-1) \|G_2\|_{\text{op}} (\|G_1\|_{\text{op}} + \|G_2\|_{\text{op}} + 1)]. \quad (34)$$

The precision then cannot achieve the Heisenberg limit if there exists  $\{\tilde{K}_j\}$  such that  $G_2 = 0$ .

### III. STATE OPTIMIZATION

The state optimization is the first step in the design of optimal schemes for quantum metrology. In the asymptotic regime, a natural target function for the optimization is the QFI, or the CFI when the measurement is fixed. Both analytical and numerical methods have been used in the state optimization. If the system is simple or possesses some special properties that can facilitate the optimization, the analytical approaches can be applied. For general complex systems numerical methods typically need to be employed.

Given a quantum channel,  $\mathcal{E}_x$ , the optimal state that achieves the channel QFI, or equivalently the optimal state that saturates the channel fidelity,  $f_{\text{qc}}(\mathcal{E}_x, \mathcal{E}_{x+\delta x})$ , can be obtained through the dual optimization of the problem in Eq. (19) [87]. Specifically, given  $\mathcal{E}_x(\rho) = \sum_{i=1}^m K_i(x) \rho K_i^\dagger(x)$ , we can define a quantum metrology matrix,  $M$ , which is a  $m \times m$  matrix with the  $ij$ th entry given by

$$M_{ij}(x_1, x_2) := \langle \psi_{\text{SA}} | K_i(x_1) K_j(x_2) | \psi_{\text{SA}} \rangle, \quad (35)$$

where  $|\psi_{\text{SA}}\rangle$  is the initial probe state of the system+ancilla and

$$\langle \psi_{\text{SA}} | K_i(x_1) K_j(x_2) | \psi_{\text{SA}} \rangle = \text{Tr}[\rho_s K_i(x_1) K_j(x_2)]$$

with  $\rho_s = \text{Tr}_A(|\psi_{\text{SA}}\rangle\langle\psi_{\text{SA}}|)$ . Given any pure input state the fidelity between the output states of two extended

channel,  $\rho_{x_1} = \mathcal{E}_{x_1} \otimes \mathbf{I}(|\psi_{\text{SA}}\rangle\langle\psi_{\text{SA}}|)$  and  $\rho_{x_2} = \mathcal{E}_{x_2} \otimes \mathbf{I}(|\psi_{\text{SA}}\rangle\langle\psi_{\text{SA}}|)$ , equals to the trace norm of the quantum metrology matrix, i.e.,

$$f(\rho_{x_1}, \rho_{x_2}) = \text{Tr} \sqrt{\sqrt{\rho_{x_1}} \rho_{x_2} \sqrt{\rho_{x_1}}} = \|M(x_1, x_2)\|_{\text{tr}}, \quad (36)$$

here  $\|M(x_1, x_2)\|_{\text{tr}} := \text{Tr} \sqrt{MM^\dagger}$ , which equals to the sum of singular values of  $M$ . The QFI of the output state can then be obtained as

$$F_x = \lim_{\delta x \rightarrow 0} \frac{8(1 - \|M(x, x + \delta x)\|_{\text{tr}})}{\delta x^2}. \quad (37)$$

The trace norm of a matrix can be efficiently calculated via the semidefinite programming as [87]

$$\begin{aligned} \|M\|_{\text{tr}} &= \min \frac{1}{2} \text{Tr}(P + Q), \\ \text{s.t. } &\begin{pmatrix} P & M^\dagger \\ M & Q \end{pmatrix} \geq 0, \end{aligned} \quad (38)$$

where  $P, Q$  are two Hermitian matrices. With the above formulation, the optimal state can then be obtained by minimizing  $\|M\|_{\text{tr}}$  through the following semi-definite programming

$$\begin{aligned} \min_{\rho_s} \|M\|_{\text{tr}} &= \min \frac{1}{2} \text{Tr}(P + Q), \\ \text{s.t. } &\begin{cases} \begin{pmatrix} P & M^\dagger \\ M & Q \end{pmatrix} \geq 0, \\ \rho_s \geq 0, \\ \text{Tr}(\rho_s) = 1. \end{cases} \end{aligned} \quad (39)$$

Any  $|\psi_{\text{SA}}\rangle$  that has the reduced state equals to  $\rho_s$  outputted from the semi-definite programming is an optimal probe state. This semi-definite programming is exactly the dual of the semi-definite programming in Eq. (19) and strong duality holds, the optimal values of both semi-definite programming give the channel fidelity.

The fact that the initial state enters  $M$  linearly is essential for the formulation of the semi-definite programming in Eq. (39). As a contrast, if the fidelity is calculated directly as

$$f = \text{Tr} \sqrt{\sqrt{\rho_{x_1}} \rho_{x_2} \sqrt{\rho_{x_1}}} \quad (40)$$

with  $\rho_x = \mathcal{E}_x \otimes \mathbf{I}(|\psi_{\text{SA}}\rangle\langle\psi_{\text{SA}}|)$ , the initial state then enters in quadratically, which cannot be computed directly with the semi-definite programming.

The formula in Eq. (37) also holds without the ancillary system when the input state is a pure state,  $|\psi_s\rangle$ . If the optimal value in Eq. (39) can be attained with a pure  $\rho_s$ , it then indicates that the channel QFI can be achieved without the ancillary system, i.e., the ancillary system does not help improve the precision in this case. This happens if all the operators  $K_i^\dagger(x_1) K_j(x_2)$  commute with each other [87], i.e.,

$$[K_i^\dagger(x_1) K_j(x_2), K_p^\dagger(x_1) K_l(x_2)] = 0 \quad (41)$$



for any subscript  $i, j, p, l$ , for such channels the optimal value in Eq. (39) can always be attained with a pure  $\rho_s$  [87], the ancillary system thus does not help improve the precision limit. In particular, the unitary channel, the phase estimation with the dephasing noise along the same direction or the phase estimation along the Z direction with the noises along the X and Y directions, all satisfy this condition, hence the ancillary system does not help improve the precision limit for these channels in the case of single-parameter estimation [87]. For example, for the dephasing channel

$$\mathcal{E}_x(\cdot) = K_1(\cdot)K_1 + K_2(\cdot)K_2 \quad (42)$$

with  $K_1 = \sqrt{p}e^{-ix\sigma_z}$  and  $K_2 = \sqrt{1-p}\sigma_z e^{-ix\sigma_z}$ , it is easy to check that

$$\left[ K_i^\dagger(x_1)K_j(x_2), K_p^\dagger(x_1)K_l(x_2) \right] = 0 \quad (43)$$

for any subscript  $i, j, p, l \in \{1, 2\}$ , the ancillary system thus can not help improving the precision limit in this case. This example is first recognized in [11] through direct comparison.

When the dimension of the system gets large, the semi-definite programming becomes computationally hard. It is then difficult to obtain the optimal state in the general case. However, for some special case, it is still possible to obtain the optimal state analytically.

### A. Analytical optimization

Analytical optimizations are difficult to perform in most cases. In general the complexity for the calculation of the QFI is equivalent to the diagonalization of the density matrix, which grows exponentially with the number of particles. However, there still exist some cases that the analytical optimization is possible. The simplest case is the unitary parameterization with  $\exp(-ixH)$ , where the optimal state can be analytically obtained [4] as the equal superposition of two eigenstates that corresponds to the maximal and minimal eigenvalues of  $H$  respectively.

The linear Mach-Zehnder interferometer (MZI) is another important scenario that the analytical state optimization has been studied. An optical MZI consists of two beam splitters and a phase shift as illustrated in Fig. 3(a). This can be modeled as the SU(2) interferometer, of which the parameterization process is  $U_{\text{mz}} = \exp(-i\phi J_y)$ , where  $J_y = \frac{1}{2i}(a^\dagger b - ab^\dagger)$  is a Schwinger operator with  $a$  ( $a^\dagger$ ) and  $b$  ( $b^\dagger$ ) as the annihilation (creation) operators for two boson modes respectively (the other two Schwinger operators are  $J_x = \frac{1}{2}(a^\dagger b + ab^\dagger)$  and  $J_z = \frac{1}{2}(a^\dagger a - b^\dagger b)$  [88]). In practice, the input states in the two modes are typically separable, which significantly reduce the state space for the optimization. This space can be further reduced when additional restrictions are invoked. For example, if the probe state in one import is restricted to be an odd or even state, then the maximal

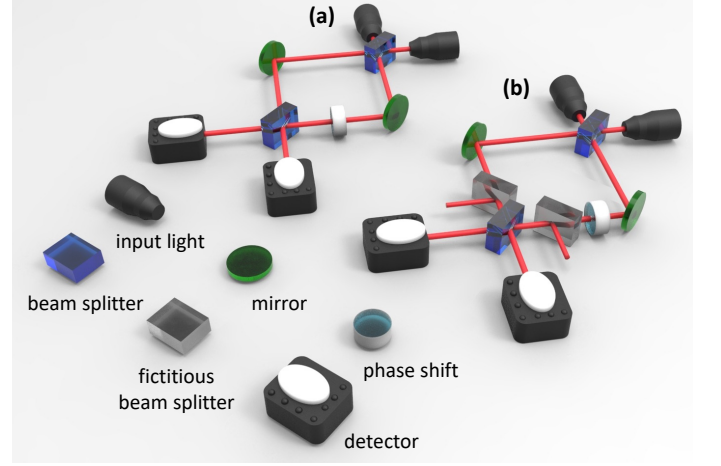


FIG. 3. (a) Scheme for a general optical Mach-Zehnder interferometer for quantum phase estimation, which consists of two beam splitters and a phase shift. (b) Scheme for the lossy Mach-Zehnder interferometer in which the photon loss in each arm is modeled by a fictitious beam splitter.

QFI can be achieved when the states of the two modes satisfy the phase-matching condition [89], which forms a basis for the state optimization in the MZI [89–91]. In practice, the phase of the input states require extra resources to identify, such as an external phase reference. Without these extra resources, the phase averaged states are more suitable in practice [92].

When the state of one mode is the coherent state ( $|\alpha\rangle$ ), Caves [88] found that by injecting the squeezed vacuum state,  $|\xi\rangle = e^{\frac{1}{2}(\xi^* a^2 - \xi a^{\dagger 2})}|0\rangle$  (here  $|0\rangle$  refers to the vacuum state and  $\xi$  the squeezing parameter), in the other mode, the standard quantum limit can be surpassed. Lang and Caves [93] further investigated this problem and showed that the squeezed vacuum state is actually optimal. It is shown by expressing the QFI in terms of the variance of the momentum as  $F_\phi = 2|\alpha|^2\langle\Delta^2\hat{p}\rangle + N_b$ , where  $\langle\Delta^2\hat{p}\rangle := \langle\hat{p}^2\rangle - \langle\hat{p}\rangle^2$  with  $\hat{p} = \frac{1}{\sqrt{2}i}(b - b^\dagger)$  and  $\langle\cdot\rangle := \text{Tr}(\cdot\rho)$  denotes the expected value,  $N_b$  is the photon number in the second mode. It can be seen that the maximal  $F_\phi$  is obtained when the variance of the momentum in the second mode is maximal. By utilizing the inequalities

$$\langle\Delta^2\hat{p}\rangle + \langle\Delta^2\hat{x}\rangle \leq \langle\hat{p}\rangle^2 + \langle\hat{x}\rangle^2 = 2N_b + 1, \quad (44)$$

$$(\langle\Delta^2\hat{p}\rangle - \langle\Delta^2\hat{x}\rangle)^2 \leq 4N_b(N_b + 1), \quad (45)$$

where  $\hat{x} = \frac{1}{\sqrt{2}}(b + b^\dagger)$  is the position operator of the second mode, one can obtain

$$2\langle\Delta^2\hat{p}\rangle \leq 2\sqrt{N_b(N_b + 1)} + 2N_b + 1, \quad (46)$$

<sup>2</sup> The Planck units ( $\hbar = 1$ ) is applied here. The other mode is for the coherent state  $|\alpha\rangle$ .

which leads to the maximum QFI

$$F_{\phi, \max} = 2N_a N_b + N_a + N_b + 2N_a \sqrt{N_b(N_b + 1)}. \quad (47)$$

This maximal QFI can be achieved with the squeezed vacuum state. Hence, when one import is fixed to be the coherent state, the squeezed vacuum state is optimal for the other port. However, the optimal state may not be unique. The existence and the properties of other optimal states need further investigation.

Lang and Caves [94] also studied the optimal state when the input state of the other import is fixed to be the squeezed vacuum state. Interestingly, the optimal state in this case is also a squeezed vacuum state. These two squeezed states need to have opposite values of  $\xi$  to satisfy the phase-matching condition.

In the case of the Bayesian estimation where the priori information of the phase is a flat distribution, it is also possible to perform the state optimization analytically. For instance, Berry and Wiseman [95, 96] studied the state optimization in the MZI [97]. The target function they used is the Holevo phase variance [98]  $S^{-2} - 1$  with

$$S = \left| \int_{-\pi}^{\pi} p(\phi) e^{i\phi} d\phi \right| \quad (48)$$

representing the sharpness of the phase distribution. For a fixed photon number, the optimal input state, which maximizes  $S$ , is given by [95, 96]

$$\sqrt{\frac{2}{N+2}} \sum_{m=-N/2}^{N/2} \sin\left(\frac{(2m+N+2)\pi}{2(N+2)}\right) |m\rangle, \quad (49)$$

where  $|m\rangle$  is the eigenstate of  $J_y$  for a fixed  $N$  with the eigenvalue  $m$ .

Apart from the direct optimization, the convex optimization has also been widely used due to the convexity of the QFI as [99, 100]

$$F_x(a\rho_1 + (1-a)\rho_2) \leq aF_x(\rho_1) + (1-a)F_x(\rho_2) \quad (50)$$

with  $a \in [0, 1]$ . The convexity of the QFI indicates that the maximal QFI can always be attained by a pure state. Since a mixed state can always be expressed as a convex combination of pure states as  $\rho = \sum_i p_i |\psi_i\rangle\langle\psi_i|$  with  $\sum_i p_i = 1$ , we then have have

$$\begin{aligned} F_x[\mathcal{E}_x(\rho)] &\leq \sum_i p_i F_x[\mathcal{E}_x(|\psi_i\rangle\langle\psi_i|)] \\ &\leq \max_i F_x[\mathcal{E}_x(|\psi_i\rangle\langle\psi_i|)]. \end{aligned} \quad (51)$$

With this convexity, Takeoka et al. [101] proved a no-go theorem for the MZI. This no-go theorem states that with the unknown phase shifts in both arms of the MZI, which is the case for the gravitational wave detection, the scaling of the precision cannot go beyond the standard quantum limit if the input of one import is vacuum.

Although the convexity of the QFI implies the optimal state is pure in general, in some specific scenarios the optimization within the mixed states could still be meaningful. In 2011 Modi et al. [102] studied the parameter estimation in terms of quantum circuits in which the initial states are prepared via the Hadamard and Control-Not gates from mixed qubit states. The state optimization in this case is performed directly from the analytical expression of the QFI. Fiderer, Fraïsse and Braun [103] considered the unitary parameterization where the initial state is prepared via unitary operations on a fixed mixed state, namely,  $\rho_{\text{in}} = U\rho_{\text{fix}}U^\dagger$  with  $U$  as any unitary operator and  $\rho_{\text{fix}}$  a fixed mixed state. The state then goes through a unitary parametrization as  $\rho = U_x\rho_{\text{in}}U_x^\dagger$ , where  $U_x$  is the unitary operator encodes the parameter. In this case, the state optimization is restricted to the state space that has the same spectrum as  $\rho_{\text{fix}}$ . Denote the spectral decomposition of  $\rho_{\text{fix}}$  as  $\rho_{\text{fix}} = \sum_{i=1}^d \lambda_i |\lambda_i\rangle\langle\lambda_i|$  with  $d$  the dimension of the density matrix, and  $\lambda_i$  is ordered as  $\lambda_1 \geq \dots \geq \lambda_d$ . Utilizing the operator  $\mathcal{H}$ , the optimal initial state is proved to be in the form  $\rho_{\text{in, opt}} = \sum_{i=1}^d \lambda_i |\phi_i\rangle\langle\phi_i|$  with

$$|\phi_i\rangle = \begin{cases} \frac{1}{\sqrt{2}}(|\mathcal{H}_i\rangle + |\mathcal{H}_{d-i+1}\rangle), & \text{if } 2i < d+1, \\ |\mathcal{H}_i\rangle, & \text{if } 2i = d+1, \\ \frac{1}{\sqrt{2}}(|\mathcal{H}_i\rangle - |\mathcal{H}_{d-i+1}\rangle), & \text{if } 2i > d+1. \end{cases} \quad (52)$$

Here  $|\mathcal{H}_i\rangle$  is an eigenstate of  $\mathcal{H}$  with  $\mathcal{H}$  the generator Hamiltonian of  $U_x$  defined as

$$\mathcal{H} = i(\partial_x U_x^\dagger) U_x = -iU_x^\dagger (\partial_x U_x). \quad (53)$$

$\mathcal{H}_i|\mathcal{H}_i\rangle = h_i|\mathcal{H}_i\rangle$  with the eigenvalue,  $h_i$ , arranged in decreasing ordered as  $h_1 \geq \dots \geq h_d$ , then the maximal QFI is

$$F_{x, \text{opt}} = \frac{1}{2} \sum_{i=1}^d c_{i, d-i+1} (h_i - h_{d-i+1})^2, \quad (54)$$

where  $c_{i, j} = 0$  if  $\lambda_i = \lambda_j = 0$  and  $(\lambda_i - \lambda_j)^2/(\lambda_i + \lambda_j)$  for others.

In the case that the generator Hamiltonian of  $U_x$  is time-dependent and controllable, i.e.,  $H = H_x(t) + H_c(t)$ , where  $H_x(t)$  depends on the unknown parameter  $x$  and  $H_c(t)$  is the control Hamiltonian. They further found an upper bound of the QFI (denoted by  $F_{\text{up}}$ ),

$$F_{\text{up}} = \frac{1}{2} \sum_{i=1}^d c_{i, d-i+1} \left[ \int_0^t (\mu_i - \mu_{d-i+1}) d\tau \right]^2, \quad (55)$$

where  $\mu_i = \mu_i(t)$  is an eigenvalue of  $\partial_x H_x(t)$  with corresponding eigenstate  $|\mu_i(t)\rangle$  with  $\mu_i$  arranged in decreasing ordered,  $\mu_1 \geq \dots \geq \mu_d$ . The optimal initial state that attains this upper bound is  $\rho_{\text{in, opt}} = \sum_{i=1}^d \lambda_i |\phi'_i\rangle\langle\phi'_i|$ , where

$$|\phi'_i\rangle = \begin{cases} \frac{1}{\sqrt{2}}(|\mu_i(0)\rangle + |\mu_{d-i+1}(0)\rangle), & \text{if } 2i < d+1, \\ |\mu_i(0)\rangle, & \text{if } 2i = d+1, \\ \frac{1}{\sqrt{2}}(|\mu_i(0)\rangle - |\mu_{d-i+1}(0)\rangle), & \text{if } 2i > d+1. \end{cases} \quad (56)$$

Correa et al. [104] studied the optimal probe state for fully thermalized thermometers, which are in equilibrium state with the reservoir. Assuming the probe is a  $N$ -dimensional system, they found the optimal thermalized state,  $\rho = e^{-\beta H}/Z$ , requires the Hamiltonian to be an effective two-level system with a highly degenerate excited state and a specific temperature-dependent gap, here  $\beta = k_B T$  with  $k_B$  as the Boltzmann constant and  $T$  as the temperature. Denote the Hamiltonian as  $H = \sum_{i=0}^{N-1} E_i |E_i\rangle\langle E_i|$ , then the optimal energy structure needs to satisfy

$$(E_i - E_j) [E_i + E_j - 2(\langle H \rangle + T)] = 0, \quad (57)$$

for any  $i$  and  $j$  with  $\langle H \rangle = \frac{1}{Z} \sum_{i=0}^{N-1} E_i e^{-\beta E_i}$ , which is equivalent to  $E_i = E_j$  or  $E_i + E_j = 2(\langle H \rangle + T)$ . This condition implies that the optimal structure is a degenerate two-level system with the energy gap  $2(\langle H \rangle + T)$ . The temperature dependence of the optimal energy gap means a tunable degenerate two-level system is required in this scheme and the measurement has to be performed adaptively.

The analytical form may also be identified when the state is restricted to be Gaussian. In 2006, Monras [105] studied the case of a single mode Gaussian state under the unitary channel,  $\exp(-ixa^\dagger a)$ . They found that the squeezed vacuum state is optimal in this case. Šafránek and Fuentes [106] further considered several specific cases including the estimation of a unitary channel that combines the phase-change, squeezing, as well as the generalized two-mode squeezing and mode-mixing channels. They provided the optimal states by the direct calculation of the QFI with analytical optimizations.

Knysh et al. [107] developed a method to identify the optimal probe states for noisy dynamics in the asymptotic limit, i.e., with an asymptotically large number of qubits or photons. They mapped the problem of identifying the optimal states to that of finding the ground state of a quantum-mechanical particle in a 1D potential, where the form of the potential can be determined from the type of the noise. With this method, they identified the optimal probe states for various noisy dynamics, including both individual and collective dephasing, relaxation and excitation, as well as combinations of the above noises. For typical noisy dynamics the optimal probes are found to approach a Gaussian profile in the asymptotic limit [107].

## B. Semi-analytical optimization

The search of optimal states for noisy dynamics is much more difficult in general. Most noisy dynamics are described in terms of the differential equations and in many cases they cannot be solved analytically, which makes the analytical state optimization impossible. In the case that the analytical solutions of the density matrix, or the QFI, can be obtained, the feasibility of the

analytical optimization is still not promised. Nevertheless, some analytical expressions are definitely useful for the optimization, which leads to the semi-analytical optimization.

Due to the convexity of the QFI, many methods in the convex optimization have been successfully applied in the state optimization. It has been applied to the lossy MZI illustrated in Fig. 3(b), where the photon loss in the optical MZI is modeled by the fictitious beam splitter. Dorner, Demkowicz-Dobrzanski et al. [108, 109] studied the state optimization in a lossy MZI where one or two arms suffer the photon losses, as illustrated in Fig. 3(b). The input state,  $|\psi_{\text{in}}\rangle$ , is taken as a two-mode pure state with fixed total photon number ( $N$ ),

$$|\psi_{\text{in}}\rangle = \sum_{k=0}^N c_k |k, N-k\rangle, \quad (58)$$

where  $|k, N-k\rangle$  is the two-mode Fock state and  $c_k$  is a complex coefficient. In the case that only one arm suffers the photon loss, the QFI can be obtained directly, which is shown to be a concave function of  $\{|c_k|^2\}$ . This means that the local maximum of the QFI is also the global maximum. The optimization can be written as

$$\begin{aligned} \min & -F_x(\{|c_k|^2\}) \\ \text{s.t.} & |c_k|^2 \geq 0. \end{aligned} \quad (59)$$

The interior-point method with the logarithmic barrier function is then used to numerically locate the optimal state [110]. The results show that in the case of  $N = 10$ , the optimal state for a small loss rate is a N00N-type state  $c_0|0N\rangle + c_N|N0\rangle$ , which, when the loss rate is 0, reduces to the N00N state,  $\frac{1}{\sqrt{2}}(|0N\rangle + |N0\rangle)$ . It is also found that the performance of the state  $c_k|k, N-k\rangle + c_N|N0\rangle$  with the optimal coefficient  $c_k$  and optimal  $k$  is very close to the optimal state in a wide regime of the loss rate.

When equal photon losses exist in both arms, the QFI is not easy to obtain. Instead, an upper bound of the QFI,  $F_x(\sum_i p_i |\psi_i\rangle\langle\psi_i|) \leq \sum_i p_i F_x(|\psi_i\rangle\langle\psi_i|)$ , has been used as the target function for the state optimization. Again by utilizing the interior-point methods, it is found that the N00N-type state is optimal for  $N < 10$ . In the case that  $N = 10$ , the standard N00N state is optimal for small losses and with the increase of the loss rate the performance of the state [95, 96, 111]

$$\sqrt{\frac{2}{N+2}} \sum_{k=0}^N \sin\left(\frac{(k+1)\pi}{N+2}\right) |k, N-k\rangle \quad (60)$$

is very close to the optimal one. Knysh et al. [112] also studied the state optimization in the lossy MZI with the input state described in Eq. (58). They considered the case where only one arm has photon loss and derived an upper bound on the QFI as  $4(1-R)N/R$ , where  $R$  is the reflectivity of the fictitious beam splitter. The optimal state is then obtained by minimizing the difference between the upper bound and the QFI.



### C. Numerical optimization

Compared to the analytical optimization, the numerical approaches can be applied to more general scenarios. Although most searching algorithms can be used in the state optimization, the algorithms typically can only be applied to systems with limited sizes due to the curse of the dimensionality. One way to solve this problem is to manually reduce the search space. For example, Fröwis et al. [113] has chosen a subspace to perform the optimization. They considered the frequency estimation of a collective spin system suffering the dephasing noise. The system Hamiltonian is  $H = S_z := \frac{1}{2} \sum_{i=1}^N \sigma_z^{(i)}$ , where  $\sigma_z^{(i)}$  is the Pauli Z matrix for the  $i$ th spin and  $N$  is the number of spins. Both the local and collective dephasing have been studied. To reduce the search space, the states are restricted to the form

$$|\psi\rangle = \sum_{m=-J}^J c_m |J, m\rangle, \quad (61)$$

where  $|J, m\rangle$  is the Dicke state with  $J = N/2$ . Such state can be characterized by  $\mathbf{c} = (c_{-J}, \dots, c_J)$ . With this ansatz, the search space reduces to the state space with the maximum angular momentum  $J$ . It can be further reduced by assuming  $c_m$  is real and positive, and  $c_m = c_{-m}$  as the dynamics is unchanged under the collective spin flipping,  $\sigma_x^{\otimes N}$ .

Within this subspace, Fröwis et al. applied the Nelder-Mead algorithm [114] to perform the state optimization that maximizes  $F_x/t$ . The Nelder-Mead algorithm is a gradient-free search method. The flow chart of the Nelder-Mead algorithm to locate the minimum target function in the case of the state optimization is shown in Fig. 4, which includes the operations of the reflection, expansion, contraction and shrink. The first step of this algorithm is to take  $n+1$  states  $\{\mathbf{c}_1, \dots, \mathbf{c}_{n+1}\}$  and calculate the objective function

$$f_i = -\frac{1}{T} F_x(\mathbf{c}_i, T) \quad (62)$$

at a given time  $T$ , order them as  $f_1 \leq f_2 \leq \dots \leq f_{n+1}$ . Next, calculate the reflection state  $\mathbf{c}_r = \bar{\mathbf{c}} + a_r(\bar{\mathbf{c}} - \mathbf{c}_{n+1})$ , here  $a_r > 0$  is the reflection coefficient and  $\bar{\mathbf{c}} = \frac{1}{n} \sum_{i=1}^n \mathbf{c}_i$ , which leads to an updated objective function  $f_r$ . The states are then updated based on the relation between  $f_r$  and the values of the existing objective functions as following:

- if  $f_1 \leq f_r < f_n$ , replace  $\mathbf{c}_{n+1}$  with  $\mathbf{c}_r$  and start over;
- if  $f_r < f_1$ , let  $\mathbf{c}_e = \bar{\mathbf{c}} + a_e(\mathbf{c}_r - \bar{\mathbf{c}})$ , and replace  $\mathbf{c}_{n+1}$  with  $\mathbf{c}_r$  ( $\mathbf{c}_e$ ) if  $f_e \geq f_r$  ( $f_e < f_r$ ). This is called the expansion step.
- if  $f_n \leq f_r < f_{n+1}$ ,  $\mathbf{c}_{oc} = \bar{\mathbf{c}} + a_c(\mathbf{c}_r - \bar{\mathbf{c}})$ , and if  $f_r \geq f_{n+1}$  let  $\mathbf{c}_{ic} = \bar{\mathbf{c}} - a_c(\bar{\mathbf{c}} - \mathbf{c}_{n+1})$ . Replace  $\mathbf{c}_{n+1}$  with  $\mathbf{c}_{ic}$  (or  $\mathbf{c}_{oc}$ ) if  $f_{ic} < f_{n+1}$  ( $f_{oc} \leq f_r$ ). This

is called the contraction step. If  $f_{ic}$  or  $f_{oc}$  fails to satisfy the conditions, then replace all the states as  $\mathbf{c}_i = \mathbf{c}_1 + a_s(\mathbf{c}_i - \mathbf{c}_1)$  and start over.

The algorithm stops when  $\Delta f = f_{n+1} - f_1 < \epsilon$  where  $\epsilon$  is a given precision. In this algorithm, the coefficients  $a_e > \max\{1, a_r\}$  and  $0 < a_c, a_s < 1$ . A usual set of coefficients is  $a_r = 1, a_e = 2, a_c = a_s = 1/2$ .

Utilizing the Nelder-Mead algorithm, Fröwis et al. [113] performed the numerical optimization for the estimation of the frequency up to 70 qubits, where the dynamics of the system is described by the master equation with the dephasing

$$\partial_t \rho = -i[\omega S_z, \rho] + \frac{\gamma}{2} \sum_i (\sigma_z^{(i)} \rho \sigma_z^{(i)} - \rho) \quad (63)$$

with  $\omega$  the frequency to be estimated. The numerical result suggests that although the optimal one-axis twisted spin-squeezed state shows a very good performance, it is still not exactly optimal up to  $N \approx 70$ . It indicates that the spin squeezed state is not necessary optimal for the frequency estimation when the number of qubits is finite, although asymptotically certain type of the spin squeezed state is optimal [107, 115]. At the presence of the collective dephasing

$$\partial_t \rho = -i[\omega S_z, \rho] - \frac{\gamma}{1 - e^{-\gamma t}} [S_z, [S_z, \rho]] \quad (64)$$

with  $\omega$  the frequency to be estimated. The numerical result suggests that the Greenberger-Horne-Zeilinger state  $\frac{1}{\sqrt{2}}(|\frac{N}{2}, -\frac{N}{2}\rangle + |\frac{N}{2}, \frac{N}{2}\rangle)$  is the optimal state.

In 2016 Knott [116] provided a search algorithm for the state optimization in quantum optics, which is inspired by the evolutionary algorithms. This algorithm takes the QFI as the target function. It considers a practical state preparation scenario with two optical modes. The input states in these modes are first chosen from several types of well-studied states in quantum optics, including the coherent state, squeezed vacuum state, and the Fock state, which then goes through a series of operations and then a heralding measurement is performed in one mode at the end. The operations includes the beam splitter operator, the displacement operator, a phase shift in one mode, the identity matrix and a non-unitary operator that measures the state in one mode and input a new state. The heralding measurement is the photon-number resolving detection, including 1 to 4 photons. The algorithm first randomly picks the input states, the operations and the heralding measurement from the toolbox and calculates the corresponding QFI. If it is large, it is taken as the parent and then create an offspring by making a random change in the process. If the offspring still provides a large QFI, then it is used to continue to create the next-generation offspring. Hence, this algorithm is similar to a random search algorithm. Applied to the case of a MZI with phase shifts on both arms, this algorithm finds states that outperform the squeezed vacuum state by a constant factor. However, the scaling

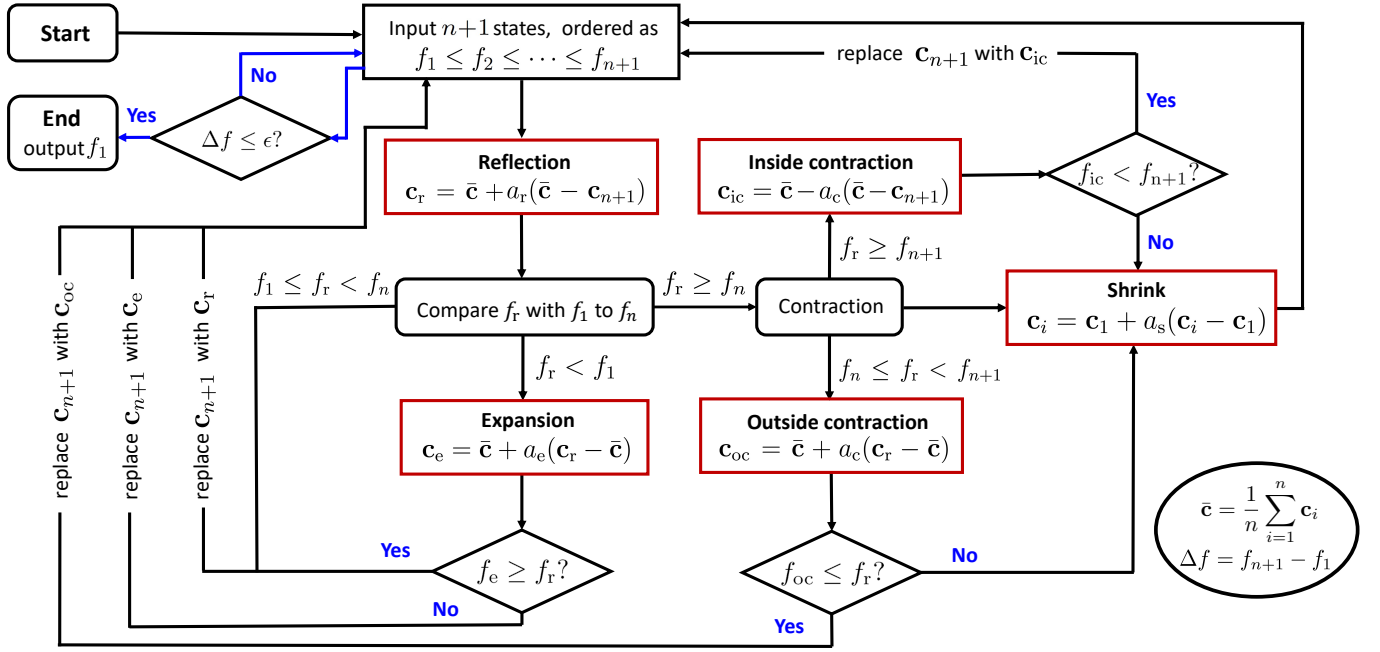


FIG. 4. Flow chart for the Nelder-Mead algorithm in the state optimization.

is still at the standard quantum limit due to the no-go theorem given in Ref. [101].

Apart from the aforementioned algorithms, many other search and optimization algorithms can be applied to the state optimization, such as the particle swarm optimization [117], the learning algorithms including the actor-critic algorithm [118] and deep deterministic policy gradient algorithm [119]. These methods are currently being merged in the QuanEstimation package<sup>3</sup> which will be thoroughly discussed in a forthcoming paper.

#### IV. OPTIMIZATION OF THE PARAMETERIZATION PROCESSES

The optimization of parameterization process is a major component for the enhancement of the precision limit. In this section we will introduce the existing optimization methods for the parameterization processes.

##### A. Quantum control

During the evolution of the parametrization process, quantum controls can be employed to alter the dynamics in a desired way which can improve the precision limit. The controls during the parametrization can either be discrete pulses or continuous wave forms.

---

#### Algorithm 1: GRAPE algorithm [120]

---

Initialize the control amplitude  $V_k(t)$  for all  $t$  and  $k$ ;  
**for** episode=1,  $M$  **do**  
  Receive initial state  $\rho_1$  (i.e.  $\rho_{in}$ );  
  **for**  $t = 1, T$  **do**  
    Evolve with the control  $\rho_{t+1} = e^{\Delta t \mathcal{L}_t} \rho_t$ ;  
    Calculate the propagators  
     $\mathcal{D}_{t+1}^t = \mathbb{1}, \mathcal{D}_t^t = e^{\Delta t \mathcal{L}_t}, \mathcal{D}_0^t = \mathcal{D}_t^t \mathcal{D}_0^{t-1}$ ;  
    **for**  $i = 1, t$  **do**  
      Calculate the propagators  
       $\mathcal{D}_{t-i}^t = \mathcal{D}_{t-i+1}^t \mathcal{D}_{t-i}^{t-1}$ ;  
    **end for**  
  **end for**  
  Save all  $\rho_t$  and  $\mathcal{D}$ ;  
  Calculate the SLD  $L_x(T)$  and QFI  $F(T)$ ;  
  **for**  $t = 1, T$  **do**  
    **for**  $k = 1, P$  **do**  
      Calculate the gradient  $\frac{\delta F(T)}{\delta V_k(t)}$ ;  
      Update control  $V_k(t) \leftarrow V_k(t) + \epsilon \frac{\delta F(T)}{\delta V_k(t)}$ ;  
    **end for**  
  **end for**  
**end for**

---

When the dynamics is unitary with a time independent Hamiltonian,  $H(x)$ , one optimal control that gives the maximal QFI is to reverse the free evolution, i.e., by adding a control Hamiltonian  $H_c = -H(x)$  [122, 123]. Since the value of the parameter is a priori unknown, in practice the controls need to be designed adaptively as  $H_c = H(\hat{x})$  with  $\hat{x}$  as the updated estimation from the accumulated data. Such optimally controlled schemes have been experimentally implemented for the estimation of

<sup>3</sup> <https://github.com/LiuJPhys/QuanEstimation>.

---

**Algorithm 2:** A3C algorithm [121]

---

```

Randomly initialize global network parameters  $\theta$  and  $\omega$ ;
for episode=1,  $M$  do
  Reset gradient:  $d\theta = 0$ ,  $d\omega = 0$ ;
  Synchronize thread-specific parameters  $\theta' \leftarrow \theta$ ,  $\omega' \leftarrow \omega$ ;
  Receive initial state  $\rho_1$  (i.e.  $\rho_{\text{in}}$ );
  for  $t = 1, T$  do
    Pick the action  $V_t$  from  $\pi(\rho_t; \theta')$ ;
    Evolve with the control and receive a reward  $r_t$  and state  $\rho_{t+1}$ ;
    Assign the value function  $V(\rho_t; \omega')$  to discount reward  $R_t$  ( $R_t = 0$  for the last time step);
  end for
  Save all  $r_t$ ,  $\rho_t$  and  $R_t$ ;
  for  $i = T, 1$  do
    Update the discount reward  $R_i \leftarrow r_i + \gamma R_{i+1}$ ;
    Update accumulate gradients  $d\theta \leftarrow d\theta + \nabla_{\theta'} \log(\pi(\rho_i; \theta')) [R_i - V(\rho_i; \omega')]$ ,  $d\omega \leftarrow d\omega + \nabla_{\omega'} [R_i - V(\rho_i; \omega')]^2$ ;
  end for
  Update the network parameters  $\theta \leftarrow \theta + d\theta$ ,  $\omega \leftarrow \omega + d\omega$ .
end for

```

---

the parameters in SU(2) operators [124, 125]. Pang and Jordan [126] considered the unitary dynamics with time-dependent Hamiltonian,  $H(x, t)$ . It is shown that the QFI for a general time-dependent unitary parameterization process is upper bounded as

$$\sqrt{F_x(t)} \leq \int_0^t h_{\max}(\tau) - h_{\min}(\tau) d\tau, \quad (65)$$

where  $h_{\max(\min)}$  is the maximum (minimum) eigenvalue of  $\partial_x H(x, \tau)$ . This upper bound can be attained by preparing the initial state as  $\frac{1}{\sqrt{2}}(|h_{\max}(0)\rangle + |h_{\min}(0)\rangle)$  and using the control to keep the state as  $\frac{1}{\sqrt{2}}(|h_{\max}(\tau)\rangle + |h_{\min}(\tau)\rangle)$  during the entire evolution, here  $|h_{\max(\min)}(\tau)\rangle$  is the eigenstate of  $\partial_x H(x, \tau)$  with respect to the eigenvalue  $h_{\max(\min)}(\tau)$ .

When the dynamics is noisy, the optimization in general can only be performed numerically. A widely used optimal quantum control method is the gradient ascent pulse engineering (GRAPE) developed by Khaneja et al. [128]. GRAPE has been employed in quantum metrology under the Markovian noisy dynamics [120, 129] where the dynamics is described by the master equation

$$\partial_t \rho = -i[H, \rho] + \sum_k \left( \Gamma_k \rho \Gamma_k^\dagger - \frac{1}{2} \{ \Gamma_k^\dagger \Gamma_k, \rho \} \right), \quad (66)$$

here the Hamiltonian takes the form

$$H = H_0 + \sum_k V_k(t) H_k, \quad (67)$$

with  $H_0$  as the free-running Hamiltonian and  $H_k$  as the  $k$ th control Hamiltonian with the time-dependent amplitude  $V_k(t)$ .

For the single-parameter estimation, the steps of the algorithm are presented in Algorithm 1, in which  $\Delta t$  is a small time interval,  $\rho_t$  ( $\mathcal{L}_t$ ) is the density matrix (superoperator) at time  $t$ . Before calculating the gradient, a full running of the evolution is required to obtain

the set of propagating superoperators  $\mathcal{D}$ , which will be used in the calculation of the gradient. The gradient in this algorithm can be obtained analytically. The corresponding specific expressions of the gradients and propagators  $\mathcal{D}$  can be found in Refs. [39, 120, 129], and the codes have been integrated into the package QuanEstimation. Besides GRAPE, Krotov's method has also been employed in the design of optimal control in quantum metrology [130].

When the size of the system increases, the simulation of the dynamics can be difficult. A hybrid quantum-classical has been proposed to deal with this issue, where the dynamics is simulated experimentally instead of numerically. Such hybrid approach has been experimentally demonstrated with the nuclear magnetic resonance [131–133]. Other hybrid variants of GRAPE have also been proposed [134–137], which can be employed in quantum metrology.

Apart from the gradient-based algorithms, learning algorithms have also been employed for the generation of optimal control in quantum metrology. For example, Xu et al. [138] used the asynchronous advantage actor-critic algorithm (A3C), a reinforcement learning algorithm, to generate optimal controls in qubit systems. The pseudocode of A3C algorithm for quantum estimation is given in Algorithm 2 and the corresponding flow chart is given in Fig. 5(a). This algorithm contains a global actor network with a distribution  $\pi(\rho_t; \theta)$  as the output and a global critic network with a value  $V(\rho_t; \omega)$  as the output. Here  $\theta$  and  $\omega$  are vectors of the network parameters and  $\rho_t$  is the density matrix at  $t$ th time step as well as the input of both networks. Before training, it assigns the task to multiple threads to enable the parallelism with local parameters  $\theta'$  and  $\omega'$  copied from the global networks. A local actor network picks the action from  $\pi(\rho_t; \theta)$  and receives a reward  $r_t$  related to the QFI( $F_t$ ), which can be the QFI itself or  $(F_t - \eta F_{\text{no},t})/F_{\text{no},t}$  [138] with  $\eta \in (0, 1]$  and  $F_{\text{no},t}$  as the QFI without the control. A local critic network generates the value function

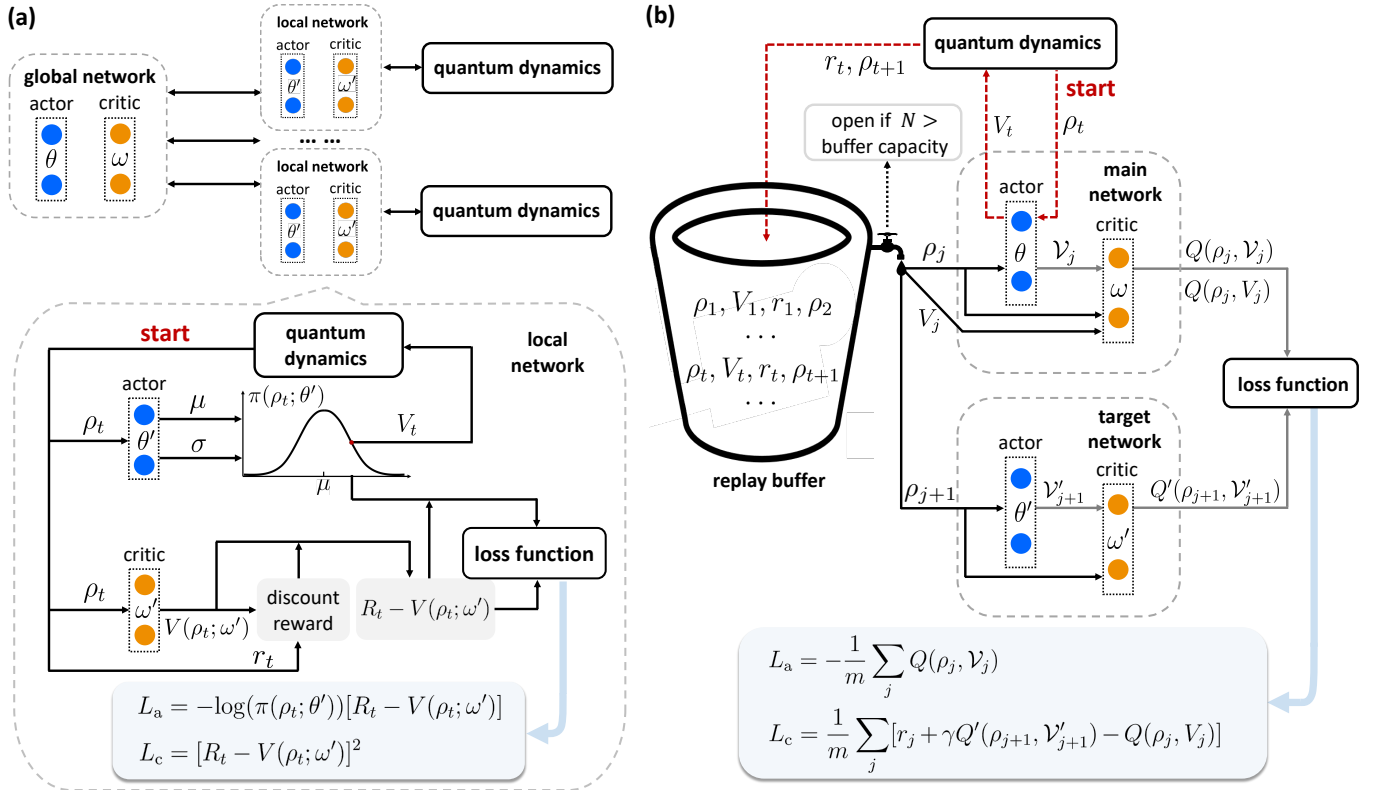


FIG. 5. (a) Flow chart for the asynchronous advantage actor-critic algorithm (A3C) in each epoch for the generation of optimal control in quantum parameter estimation. (b) Flow chart for the deep deterministic policy gradient algorithm (DDPG) in each epoch for the generation of optimal control in quantum parameter estimation. (b) is a reprinted figure with permission from [127]. Copyright (2021) by the American Physical Society.

$V(\rho_t; \omega)$ , the parameters in the global network are then updated sequentially after the final ( $T$ th) time step according to the accumulate gradients in all local networks.

The performance of A3C algorithm works well in qubit systems, especially combined with the proximal policy optimization algorithm [138]. However, it becomes hard to converge when the dimension of the system increases. In these cases, the deep deterministic policy gradient (DDPG) algorithm might be a better choice, which has been demonstrated to be feasible in the generation of optimal control for certain estimations involves multiple parameters [139]. It has also been used to enhance the spin squeezing [127]. The pseudocode of DDPG algorithm for quantum estimation is given in Algorithm 3 and the corresponding flow chart is given in Fig. 5(b). This algorithm contains two actor-critic networks which are usually referred to as the main networks and target networks, respectively. The main actor network outputs a value  $\mu(\rho_t; \theta)$ , which, by adding a random distribution  $\mathcal{N}_t$ , gives the action  $V_t$  as  $V_t = \mu(\rho_t; \theta) + \mathcal{N}_t$ . The main critic network outputs a value  $Q(\rho_t, V_t; \omega)$ , which is treated as a loss function for the update of  $\theta$ . For the sake of minimizing the correlations between samples,  $N$  sets of data  $(\rho_t, V_t, r_t, \rho_{t+1})$  are stored in a replay buffer  $\mathcal{R}$ , where  $r_t$  is the reward related to the QFI. When the

storage is finished, a random minibatch of  $m$  transitions in the buffer are put into the main and target networks during each time step, which is used to obtain the gradients with respect to  $\theta$  and  $\omega$ . The main networks are then updated accordingly. The update of the target networks are typically much slower than the main networks to avoid sharp waving of the total rewards. Feedback controls can also be used to enhance the QFI [140, 141].

For non-Markovian dynamics, recently studies have also obtained the optimal precision which can be computed with the semi-definite programming [142, 143].

## B. Quantum error correction

Quantum error correction is an important tool to battle the noises. Since the pioneer work by Peter Shor [144], general theory of quantum error correction has been developed [78, 145–149] and applied in quantum computation [150–153] and quantum communication [67, 154, 155]. Recently, the error correction has also been applied in quantum metrology for the enhancement of the precision limit [115, 156–166].



---

**Algorithm 3:** DDPG algorithm [119]

---

```

Randomly initialize main network parameters  $\theta$  and  $\omega$ ;
Synchronize target network parameters  $\omega' \leftarrow \omega$ ,  $\theta' \leftarrow \theta$ ;
Initialize replay buffer  $\mathcal{R}$ ;
for episode=1,  $M$  do
  Initialize a random distribution  $\mathcal{N}$  for action exploration;
  Receive initial state  $\rho_1$  (i.e.  $\rho_{\text{in}}$ );
  for  $t = 1, T$  do
    Take the action  $V_t = \mu(\rho_t; \theta) + \mathcal{N}_t$ ;
    Evolve with the control and receive a reward  $r_t$  and state  $\rho_{t+1}$ ;
    Store transition  $(\rho_t, V_t, r_t, \rho_{t+1})$  in  $\mathcal{R}$ ;
    if  $N >$  buffer capacity then
      Sample a random minibatch of  $m$  transitions  $\{(\rho_j, V_j, r_j, \rho_{j+1})\}$  from  $\mathcal{R}$ ;
      Calculate all  $y_j = r_j + \gamma Q'(\rho_{j+1}, V_{j+1}; \omega')$  in the minibatch;
      Calculate the gradient  $\nabla_{\theta} L_a$  with  $L_a = -\frac{1}{m} \sum_j Q(\rho_j, V_j; \omega)$ ;
      Calculate the gradient  $\nabla_{\omega} L_c$  with  $L_c = \frac{1}{m} \sum_j [y_j - Q(\rho_j, V_j; \omega)]^2$ ;
      Update main network parameters  $\theta \leftarrow \theta + \nabla_{\theta} L_a$ ,  $\omega \leftarrow \omega + \nabla_{\omega} L_c$ ;
      Update target network parameters  $\theta' \leftarrow \tau\theta + (1 - \tau)\theta'$ ,  $\omega' \leftarrow \tau\omega + (1 - \tau)\omega'$  with  $\tau$  a small weight.
    end if
  end for
end for

```

---

Given a general noisy quantum channel

$$\mathcal{E}(\rho_{\text{in}}) = \sum_{j=1}^m K_j \rho_{\text{in}} K_j^{\dagger}, \quad (68)$$

the task of quantum error correction is to find a subspace (or error-correcting code)  $\mathcal{C}$  of the Hilbert space such that for any quantum state  $\rho_c$  in the subspace, there always exists a recovery channel  $\mathcal{R}$  which can eliminate the effect of the noise, i.e.,

$$\mathcal{R}(\mathcal{E}(\rho_c)) \propto \rho_c, \quad (69)$$

where  $\rho_c$  is a state in the subspace  $\mathcal{C}$ . This is possible if each of the error (Kraus) operators  $K_i$  maps the code  $\mathcal{C}$  to undeformed and respectively orthogonal subspace, which is detectable and correctable. This forms the condition of quantum error correction [78, 146, 147], specifically,  $\mathcal{R}$  exists if and only if all the Kraus operators satisfy

$$\Pi_c K_j^{\dagger} K_l \Pi_c = c_{jl} \Pi_c, \quad (70)$$

where  $\Pi_c$  is the projective operator to the code space spanned by the code  $\mathcal{C}$  and  $c_{jl}$  is a complex constant satisfying  $c_{jl} = c_{lj}^*$ .

In quantum metrology, besides correcting the noise, a useful quantum error correction code must also protect the information of the parameter at the same time. Without loss of generality [162, 166], assume the Hamiltonian of the dynamics takes the form  $H = xG$  with  $x$  as the unknown parameter and  $G$  as the generator, and for a small time interval  $dt$  the dynamics is described by  $\mathcal{E}(U_{dt}(\rho_c))$  with  $U_{dt}(\rho_c) = e^{-iHdt} \rho_c e^{iHdt}$  and  $\mathcal{E}(\rho) = \sum_j K_j \rho K_j^{\dagger}$ . The goal of error correction is then to design a recovery operation  $\mathcal{R}$  such that  $\mathcal{R}(\mathcal{E}(U_{dt}(\rho_c)))$  is effectively unitary in the code subspace  $\mathcal{C}$  with nontrivial parametriza-

tion. Such recovery operation  $\mathcal{R}$  exists if and only if [156]

$$\begin{aligned} (1) & \Pi_c K_j^{\dagger} K_l \Pi_c = c_{jl} \Pi_c, \quad \forall j, l; \\ (2) & \max_{|\Psi\rangle \in \mathcal{C}} \langle \Delta G_{\text{eff}}^2 \rangle > 0, \end{aligned} \quad (71)$$

where  $G_{\text{eff}} = \Pi_c G \Pi_c$  is the effective generator in the code space,  $\langle \Delta G_{\text{eff}}^2 \rangle = \langle \Psi | G_{\text{eff}}^2 | \Psi \rangle - \langle \Psi | G_{\text{eff}} | \Psi \rangle^2$ . Condition (1) straightforwardly comes from Eq. (70), which ensures the existence of a recovery operation  $\mathcal{R}$ . Condition (2) requires the error-corrected dynamics depends nontrivially on the parameter  $x$  and the maximal QFI of  $x$  is non-zero.

When the noise is Markovian and the dynamics is described by the master equation as

$$\partial_t \rho = -i[H, \rho] + \sum_k \gamma_k \left( \Gamma_k \rho \Gamma_k^{\dagger} - \frac{1}{2} \{ \Gamma_k^{\dagger} \Gamma_k, \rho \} \right), \quad (72)$$

The error-correction condition can be equivalently formulated as [162, 166]

$$\begin{aligned} (1) & \Pi_c \Gamma_j \Pi_c = \lambda_j \Pi_c, \quad \forall j; \\ (2) & \Pi_c \Gamma_j^{\dagger} \Gamma_l \Pi_c = \mu_{jl} \Pi_c, \quad \forall j, l; \\ (3) & \Pi_c G \Pi_c \neq \kappa \Pi_c. \end{aligned} \quad (73)$$

Here  $\lambda_j$ ,  $\mu_{jl}$  are complex numbers and  $\kappa$  is a constant. Under the error-correction, the state in the code space evolves effectively as  $\partial_t \rho = -i[H_{\text{eff}}, \rho]$ , where  $H_{\text{eff}} = xG_{\text{eff}} = x\Pi_c G \Pi_c$ . With this noiseless evolution, the maximal QFI is achieved by choosing the initial state as  $|\psi_{\text{in}}\rangle = \frac{1}{\sqrt{2}}(|\lambda_{\text{min}}\rangle + |\lambda_{\text{max}}\rangle)$ , where  $|\lambda_{\text{min}}\rangle$  and  $|\lambda_{\text{max}}\rangle$  are the eigenstates of  $H_{\text{eff}}$  with respect to the minimum and maximum eigenvalues. And the corresponding QFI is  $F_x = t^2(\lambda_{\text{max}} - \lambda_{\text{min}})^2$ , indicating the Heisenberg limit is achieved. Denote the space spanned by the Lindblad

operators as  $\mathcal{S} = \text{span}\{\mathbf{I}, \Gamma_j, \Gamma_j^\dagger, \Gamma_j^\dagger \Gamma_l\}$ , it has been shown that the precision can reach the Heisenberg scaling if and only if  $H \notin \mathcal{S}$ , i.e., the HNLS (Hamiltonian-not-in-Lindblad-span) condition [162, 166]. When the condition holds, an explicit construction of the error-correcting code has also been provided by Zhou et al. [166]: define an inner product between two Hermitian matrices,  $A$  and  $B$ , as  $\text{Tr}(AB)$ , the Hamiltonian can then be uniquely decomposed as  $H = H_\parallel + H_\perp$ , where  $H_\parallel \in \mathcal{S}$  and  $H_\perp \perp \mathcal{S}$ , if  $G \notin \mathcal{S}$ , then  $H_\perp \perp \mathcal{S}$  is nonzero and can be written as  $H_\perp = \frac{1}{2} \|H_\perp\|_1 (\rho_0 - \rho_1)$ , where  $\rho_0$  and  $\rho_1$  are trace-one positive matrices with orthogonal support. By introducing an ancillary system,  $\mathcal{H}_A$ ,  $\rho_0$  and  $\rho_1$  can be purified as  $|C_0\rangle$  and  $|C_1\rangle$  which have orthogonal support in  $\mathcal{H}_A$ , the error correction code can then be chosen as the subspace of  $\mathcal{H}_S \otimes \mathcal{H}_A$  spanned by  $|C_0\rangle$  and  $|C_1\rangle$ .

In the quantum error correction protocol for quantum metrology, the degrees of freedom available for optimization is the error correction code. In the case of single-parameter estimation, the code optimization is to optimize  $\text{span}\{|C_0\rangle, |C_1\rangle\}$  to let the Hamiltonian has the maximum gap between the minimum and maximum eigenvalues. Using  $\lambda_{\max} - \lambda_{\min} = \text{Tr}(H_{\text{eff}} \tilde{C}) = \text{Tr}(H_\perp \tilde{C})$  with  $\tilde{C} = \rho_0 - \rho_1$ , the optimization can be formulated as [166]

$$\begin{aligned} \max \text{Tr}(\tilde{C} H_\perp) \\ \text{s.t. } \|\tilde{C}\|_{\text{op}} \leq 2, \\ \text{Tr}(\tilde{C} S) = 0, \forall S \in \mathcal{S}. \end{aligned} \quad (74)$$

Its Lagrange dual problem can be solved efficiently via semidefinite programming as

$$\begin{aligned} \min s \\ \text{s.t. } \begin{pmatrix} s\mathbf{I} & H_1 \\ H_1 & s\mathbf{I} \end{pmatrix} \geq 0 \end{aligned} \quad (75)$$

for variables  $\nu_k \in \mathbb{R}$  and  $s \geq 0$ , here  $H_1 = H_\perp + \sum_k \nu_k E_k$  and  $\{E_k\}$  is any basis of  $\mathcal{S}$ . In the multiparameter case, the code optimization is much more complicated as one needs to optimize not only the error correction code but also the input state and the final measurement. An algorithm is given by Górecki et al. [165] to tackle these problems. For the dynamics with specific noise, there also exist ancilla-free protocols to achieve the Heisenberg limit [163]. If the HNLS condition is violated, the precision can only achieve the standard quantum limit, and with approximate quantum error correction, it has been shown that the upper bound in Eq. (34), where only the first term survives, can be saturated for asymptotically large  $N$  up to an arbitrarily small error [115]. This determines the ultimate precision limit that can be achieved when the HNLS condition fails.

## V. OPTIMIZATION OF THE MEASUREMENT

Theoretically for the single-parameter estimation the quantum Cramér-Rao bound can be saturated with

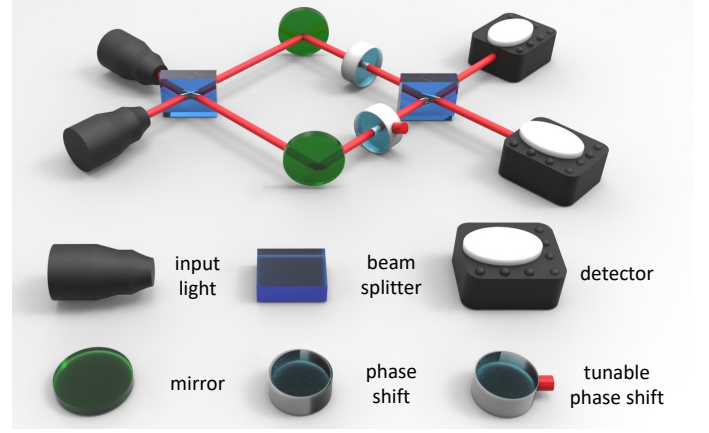


FIG. 6. Adaptive measurement scheme in MZI. In this scheme, apart from the unknown phase shift, a known tunable phase shift exists in other arm.

the projective measurement on the eigenstates of the SLD operator. However, when the size of the system increases, the eigenstates of the SLD can be hard to identify. Such measurement can also be highly nonlocal and practically challenging. In general these measurements can also depend on the value of the unknown parameter, thus can only be realized adaptively. This often requires a large amount of data processing that needs to be optimized. Here we review some optimization techniques that are employed for the local adaptive measurement, which are practically less demanding.

The adaptive measurement was first used in the optical MZI, where apart from the unknown phase shift, an additional tunable phase is introduced in the other arm in an adaptive way, as illustrated in Fig. 6. It requires many rounds of the measurement and the tunable phase needs to be adjusted in each round according to the accumulated measurement data. The major requirements of the adaptive scheme is that the precision of the known phase has to be much better than that of the phase to be estimated. In this scheme, how to tune the known phase becomes an important question as it affects both the precision of the results as well as the efficiency of the scheme.

Both online and offline optimizations have been proposed to optimize the tunable phase. In the online approach the tunable phase is adjusted through the real-time optimization based on the results of the previous rounds, and in the offline approach the adjustment of the tunable phase is given by a fixed formula which is optimized before the experiment.

Berry et al. [29, 95, 96] proposed an adaptive local measurement for the phase estimation, where the target function to maximize is taken as the sharpness function which will be specified below. Different target functions can be employed which typically converge to the variance in the asymptotic limit. In this scheme, the probe state  $|\psi_{\text{in}}\rangle$  is prepared in the form of Eq. (49) with the  $N$

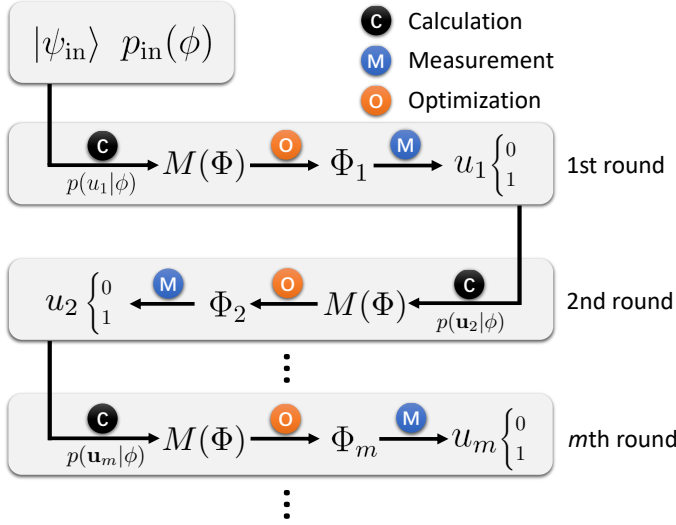


FIG. 7. Illustration of the process of an online adaptive measurement. In each round of the measurement, one needs to calculate the target function  $M(\Phi)$  based on  $p(\mathbf{u}_m|\phi)$  and then optimize it to obtain an optimal tunable phase  $\Phi_m$ , which is used to adjust the MZI. The measurement is performed with the adjusted MZI and the result is recorded. For an offline scheme, no optimization is applied during the experiment and all  $\{\Phi_N\}$  is obtained in advance.

photons. Then only one photon goes thorough the MZI in each round. The protocol is illustrated in Fig. 7. In the  $m$ th round, the target function, which is based on the conditional probability, is calculated which is used to obtain an optimal tunable phase,  $\Phi_m$ . We first show the calculation of the conditional probability given a series of measurement results. The annihilation operator in the output port of the MZI can be expressed as [95, 96]

$$a_u = a_{\text{in}} \sin \left( \frac{1}{2}(\phi - \Phi) + \frac{\pi}{2}u \right) + b_{\text{in}} \cos \left( \frac{1}{2}(\phi - \Phi) + \frac{\pi}{2}u \right), \quad (76)$$

where  $a_u$  ( $u = 0, 1$ ) is the annihilation operator for one output port of the MZI,  $a_{\text{in}}$  and  $b_{\text{in}}$  are the annihilation operators for the input modes,  $\phi$  is the unknown phase and  $\Phi$  is the tunable phase. The probability of observing a photon in  $a_0$  mode,  $p(0|\phi)$ , in the first round is then

$$p(0|\phi) = \frac{1}{N} \langle \psi_{\text{in}} | a_0^\dagger a_0 | \psi_{\text{in}} \rangle, \quad (77)$$

here  $1/N$  is the probability of picking one photon from the  $N$  photons and  $\langle \psi_{\text{in}} | a_0^\dagger a_0 | \psi_{\text{in}} \rangle$  is the probability of detecting this photon in  $a_0$  mode. Similarly,  $p(1|\phi) = \frac{1}{N} \langle \psi_{\text{in}} | a_1^\dagger a_1 | \psi_{\text{in}} \rangle$ . When the measurement result has been recorded in this round, the post-measurement state becomes

$$|\psi_{u_1}\rangle = a_{u_1} |\psi_{\text{in}}\rangle, \quad (78)$$

where  $u_1 = 0, 1$  is the result of the first round, i.e.,  $u_1 = 0$  ( $u_1 = 1$ ) means a photon is detected in  $a_0$  ( $a_1$ ) mode. Physically, the post-measurement state becomes a  $(N - 1)$ -photon state as one photon has been absorbed during the measurement, which is described by the annihilation operator on  $|\psi_{\text{in}}\rangle$ . Note that  $|\psi_{u_1}\rangle$  is *unnormalized*, the corresponding normalized state reads

$$\begin{aligned} |\tilde{\psi}_{u_1}\rangle &= \frac{1}{\sqrt{\langle \psi_{u_1} | \psi_{u_1} \rangle}} a_{u_1} |\psi_{\text{in}}\rangle \\ &= \frac{1}{\sqrt{\langle \psi_{\text{in}} | a_{u_1}^\dagger a_{u_1} | \psi_{\text{in}} \rangle}} a_{u_1} |\psi_{\text{in}}\rangle. \end{aligned} \quad (79)$$

In the next (second) round, the probability of observing a photon in  $a_{u_2}$  ( $u_2 = 0, 1$ ) is

$$\begin{aligned} p(u_2|\phi) &= \frac{1}{N-1} \langle \tilde{\psi}_{u_1} | a_{u_2}^\dagger a_{u_2} | \tilde{\psi}_{u_1} \rangle \\ &= \frac{1}{N-1} \frac{\langle \psi_{\text{in}} | a_{u_1}^\dagger a_{u_2}^\dagger a_{u_2} a_{u_1} | \psi_{\text{in}} \rangle}{\langle \psi_{\text{in}} | a_{u_1}^\dagger a_{u_1} | \psi_{\text{in}} \rangle}, \end{aligned} \quad (80)$$

where  $1/(N - 1)$  is the probability of picking a photon from the left  $N - 1$  photons. The post-measurement state can be similarly obtained.

Repeating this process, in the  $m$ th round the conditional probability  $p(u_m|\phi)$  can be expressed as

$$\begin{aligned} p(u_m|\phi) &= \frac{1}{N - (m - 1)} \langle \tilde{\psi}_{u_{m-1}} | a_{u_m}^\dagger a_{u_m} | \tilde{\psi}_{u_{m-1}} \rangle \\ &= \frac{1}{N - (m - 1)} \frac{\langle \psi_{\text{in}} | a_{u_1}^\dagger \dots a_{u_m}^\dagger a_{u_m} \dots a_{u_1} | \psi_{\text{in}} \rangle}{\langle \psi_{\text{in}} | a_{u_1}^\dagger a_{u_1} \dots a_{u_{m-1}}^\dagger a_{u_{m-1}} | \psi_{\text{in}} \rangle}, \end{aligned} \quad (81)$$

where  $a_{\mathbf{u}_m} := \prod_{i=1}^m a_{u_i}$ . The conditional probability, denoted as  $p(\mathbf{u}_m|\phi)$ , of observing a series of results,  $\mathbf{u}_m = (u_1, u_2, \dots, u_m)$ , is then

$$\begin{aligned} p(\mathbf{u}_m|\phi) &= \prod_{i=1}^m p(u_i|\phi) \\ &= \frac{(N - m)!}{N!} \langle \psi_{\text{in}} | a_{\mathbf{u}_m}^\dagger a_{\mathbf{u}_m} | \psi_{\text{in}} \rangle. \end{aligned} \quad (82)$$

Based on the conditional probability, the tunable phase,  $\Phi_m$ , can be adjusted. Suppose  $m - 1$  rounds of adaptive measurements have been carried out with the result  $\mathbf{u}_{m-1}$ . In [95, 96], the tunable phase in the  $m$ th round,  $\Phi_m$ , is obtained by maximizing the quantity

$$M_{\text{on}}(\Phi) = \sum_{u_m=0,1} p(u_m) S_{u_m}, \quad (83)$$

here  $S_{u_m}$  is the sharpness function,

$$S_{u_m} = \left| \int_{-\pi}^{\pi} p(\phi|\mathbf{u}_m) e^{i\phi} d\phi \right| \quad (84)$$

and  $p(u_m) = \int_{-\pi}^{\pi} p(u_m|\phi) p(\phi) d\phi$  is the probability of observing  $u_m$  in the  $m$ th round, here  $p(\phi)$  is the probability distribution conditional on the recorded measurement data,  $\mathbf{u}_{m-1}$ . Alternatively we can write  $p(u_m) =$

---

**Algorithm 4:** PSO algorithm [167, 168]

---

```

Initialize  $\Phi_1^{(i)}$  and  $\Delta\Phi_1^{(i)}$  for each  $i \in [1, L]$ ;
Initialize all  $\varphi_1^{(i)} = 0$ ;
for  $m = 1, M$  do
  for  $i = 1, L$  do
    Receive the adjustments of the feedback phase  $\Delta\Phi_m^{(i)}$ ;
    Calculate the objective function  $M_{\text{off}}(\{\Delta\Phi_m^{(i)}\})$ ;
    Calculate the personal best adjustments of the feedback phase  $\Delta\Phi_{m,\text{pb}}^{(i)} = \arg \left( \max_{k \in [1, m]} M_{\text{off}}(\{\Delta\Phi_k^{(i)}\}) \right)$ ;
  end for
  Compare all  $M_{\text{off}}(\{\Delta\Phi_{m,\text{pb}}^{(i)}\})$  and determine the global best adjustments of the feedback phase
   $\Delta\Phi_{m,\text{gb}} = \arg \left( \max_{i \in [1, L]} M_{\text{off}}(\{\Delta\Phi_{m,\text{pb}}^{(i)}\}) \right)$ ;
  for  $i = 1, L$  do
    Calculate  $\varphi_m^{(i)} = c_0 \varphi_{m-1}^{(i)} + \text{rand}() \cdot c_1 (\Delta\Phi_{m,\text{pb}}^{(i)} - \Delta\Phi_m^{(i)}) + \text{rand}() \cdot c_2 (\Delta\Phi_{m,\text{gb}} - \Delta\Phi_m^{(i)})$ ;
    Update the adjustments of the feedback phase  $\Delta\Phi_{m+1}^{(i)} = \Delta\Phi_m^{(i)} + \varphi_m^{(i)}$ .
  end for
end for

```

---

$p(u_m | \mathbf{u}_{m-1})$ , since it is an online scheme and all the probabilities in this round should be based on the fact that all the results in previous rounds, i.e.,  $\mathbf{u}_{m-1}$ , have already been recorded. Therefore,

$$p(u_m) = \frac{p(\mathbf{u}_m)}{p(\mathbf{u}_{m-1})}, \quad (85)$$

with

$$p(\mathbf{u}_m) = \int_{-\pi}^{\pi} p(\mathbf{u}_m | \phi) p_{\text{in}}(\phi) d\phi \quad (86)$$

as the probability of observing the result  $\mathbf{u}_m$ . Here  $p(\mathbf{u}_m | \phi)$  can be calculated as in Eq. (82) and  $p_{\text{in}}(\phi)$  is the original priori probability before the experiment. If no priori information exists, it can just be chosen as the uniform distribution, i.e.,  $p_{\text{in}}(\phi) = 1/(2\pi)$ .

The conditional probability,  $p(\phi | u_m)$ , in  $S_{u_m}$  can be obtained via the Bayes' rule,

$$p(\phi | \mathbf{u}_m) = \frac{p(\mathbf{u}_m | \phi) p_{\text{in}}(\phi)}{p(\mathbf{u}_m)}. \quad (87)$$

The sharpness function then reads

$$\begin{aligned} S_{u_m} &= \left| \int_{-\pi}^{\pi} p(\phi | \mathbf{u}_m) e^{i\phi} d\phi \right| \\ &= \frac{1}{p(\mathbf{u}_m)} \left| \int_{-\pi}^{\pi} p(\mathbf{u}_m | \phi) p_{\text{in}}(\phi) e^{i\phi} d\phi \right|. \end{aligned} \quad (88)$$

Thus

$$M_{\text{on}}(\Phi) = \frac{\sum_{u_m} \left| \int_{-\pi}^{\pi} p(\mathbf{u}_m | \phi) p_{\text{in}}(\phi) e^{i\phi} d\phi \right|}{\int_{-\pi}^{\pi} p(\mathbf{u}_{m-1} | \phi) p_{\text{in}}(\phi) d\phi}. \quad (89)$$

In the first round, the denominator of the above equation should be set to 1. The optimization is then performed

to obtain the optimal tunable phase,  $\Phi_m$ , which is used in the MZI for the  $m$ -th round. Repeating this approach, a complete online adaptive policy  $\{\Phi_m\}$  can be obtained according to the recorded results in all rounds.

Different from the online strategy where  $\{\Phi_m\}$  are determined through the real-time optimization,  $\{\Phi_m\}$  in the offline strategy are generated by formulas which are optimized before the experiment. One choice of the target function in the offline strategy, without any measurement data, is to take the average of the sharpness function over all possible trajectories of  $\mathbf{u}_m$ ,

$$M_{\text{off}}(\Phi) = \sum_{\mathbf{u}_m} \left| \int_{-\pi}^{\pi} p(\mathbf{u}_m | \phi) p_{\text{in}}(\phi) e^{i\phi} d\phi \right|. \quad (90)$$

The optimal tunable phase,  $\Phi_m$ , can then be determined by optimizing  $M_{\text{off}}(\Phi)$ , which can be performed offline. Hentschel and Sanders [167] provided an offline adaptive measurement scheme based on the particle swarm optimization (PSO) [168]. In their scheme, the tunable phase in the real experiment is updated via the rule

$$\Phi_m = \Phi_{m-1} - (-1)^{u_{m-1}} \Delta\Phi_m, \quad (91)$$

where  $u_{m-1} = 0, 1$  ( $m \geq 2$ ) is the result obtained in the  $m-1$  round experiment, and  $\Phi_1$  is set manually. With this rule, the goal of the strategy is to provide a set of good

$$\{\Delta\Phi_m\} := \{\Delta\Phi_1, \Delta\Phi_2, \dots, \Delta\Phi_M\} \quad (92)$$

via PSO algorithms, where the flow of the algorithm is given in Algorithm 4. As the number of the trajectories in Eq. (90) grows exponentially ( $\sim 2^N$ ), in practise  $M_{\text{off}}(\Phi)$  is often approximated by averaging a reasonable number of sampled trajectories [169–171]. And typically only a polynomial number of trajectories are needed to



obtain a good approximation. Peng and Fan [172] further proposed an ansatz that reduces the complexity to  $N^4$ . Experimentally, an offline scheme based on the PSO algorithm has been realized by Lumino et al. [173].

Other optimization methods, such as the genetic algorithm [174] and the differential evolution (DE) algorithm [175], have also been used in the offline adaptive measurement. Compared to the PSO algorithm, the performance of the DE algorithm is more robust, and the DE algorithm also works better with a large photon number [171].

Wiseman [176] considered the adaptive homodyne measurement scheme for the phase estimation, which was further discussed with both the semiclassical approach [177] and the quantum mechanical approach [178]. The scheme was also experimentally demonstrated by Armen et al. [179] with coherent states as the input states. In 1996, D'Ariano et al. [180] discussed the two-quadrature measurement with squeezed states as the input states. Further in 2009, Olivares et al. [181] pointed out the optimal squeezing parameter with respect to the true value of the unknown phase (or relative phase in the adaptive measurement) in the homodyne detection and invoked the Bayesian inference to update the posterior probability. Bayesian estimation based on continuously monitored environment have also been studied [182–187].

The Bayesian estimator is asymptotically unbiased and is capable to attain the quantum Cramér-Rao bound in the asymptotic limit. In 2015, Berni et al. [188] experimentally realized the adaptive homodyne measurement with the squeezed vacuum states and Bayesian inference. Wheatley et al. [189] used an adaptive homodyne measurement scheme to estimate a stochastically varying phase shift on a coherent beam utilizing the quantum smoothing techniques introduced by Tsang [190]. Wiebe and Granade [191] proposed the rejection filtering to approximate the Bayesian inference which can reduce the memory of samplings. Zheng et al. [192] experimentally applied this method to an adaptive Bayesian measurement for the optical phase estimation. Adaptive Bayesian estimation has also been experimentally applied to multiparameter estimation by Valeri et al. [193]. Recently, Fiderer et al. [194] also used the neural network for the adaptive Bayesian quantum estimation. Joint measurements on conjugate observables have also been demonstrated [195].

We note that in practice the choices of the measurement can be very limited. For example, in optical systems, the typical measurements are photon counting, homodyne measurement, displacement measurement where the successful rate is also limited by the hardware efficiency. In practise, it is important to include the practical constraints in the optimization.

## VI. SUMMARY

The optimization of the schemes is crucial to gain quantum advantages in quantum metrology. Here we re-

viewed the recent development of the optimizations in the three steps of the schemes in quantum metrology: preparation (Sec. III), parameterization (Sec. IV) and measurement (Sec. V). In the process of state preparation, analytical, semi-analytical and numerical approaches are reviewed. In the parameterization process, both quantum control and quantum error correction techniques are presented. In the measurement, the optimizations of the adaptive measurement and other scenarios are summarized. In practice, typically the optimization of the parameterization process is first performed which identifies the optimal control that leads to the channel with the maximal quantum channel Fisher information, the optimal probe state is then identified according to the obtained channel, finally the optimal measurement is determined based on the output probe state.

A practical challenge for the implementation of the optimal schemes, just as in all other quantum technologies, is the curse of the dimensionality. Although some techniques presented can reduce the complexity by restricting to a subspace, this either requires certain symmetries or loses the global optimality. Practical techniques that can provide optimal schemes for intermediate number—from dozens to thousands—of particles are highly desired. Another practical challenge is that the systems in practise may not be well characterized. This can be partially addressed in terms of the nuisance parameters [196, 197] or with a full multi-parameter quantum estimation [39, 72, 198]. The tradeoff between the optimality and the robustness of the schemes, however, requires further studies. The optimal scheme in the finite regime [199–202], even for the single-parameter estimation, is still not well-understood and there are plenty of rooms for optimizations.

Finally we note that these techniques are not only useful in quantum metrology, but can also be adopted in various other applications, such as quantum process tomography, quantum channel discrimination, variational quantum eigensolver, quantum verification, etc., and could serve as a bridge among different applications.

## Acknowledgements

The authors would like to thank Jinfeng Qin, Huai-Ming Yu and Yu-Qian Xu for helpful discussions. This work was supported by National Natural Science Foundation of China through Grant No. 11805073, No. 12175075 and the Research Grants Council of Hong Kong through the Grant No. 14307420.

## Conflict of Interest

The authors declare no conflict of interest.

## Keywords

quantum parameter estimation, quantum Cramér-Rao bound, quantum control, optimization

- 
- [1] C. W. Helstrom, *Quantum Detection and Estimation Theory*, New York: Academic, **1976**.
- [2] A. S. Holevo, *Probabilistic and Statistical Aspects of Quantum Theory*, Amsterdam: North-Holland, **1982**.
- [3] V. Giovannetti, S. Lloyd, L. Maccone, *Nat. Photon.* **2011**, *5* 222.
- [4] V. Giovannetti, S. Lloyd, L. Maccone, *Phys. Rev. Lett.* **2006**, *96* 010401.
- [5] P. M. Anisimov, G. M. Raterman, A. Chiruvelli, W. N. Plick, S. D. Huver, H. Lee, J. P. Dowling, *Phys. Rev. Lett.* **2010**, *104* 103602.
- [6] S. L. Braunstein, C. M. Caves, *Phys. Rev. Lett.* **1994**, *72* 3439.
- [7] M. G. A. Paris, *Int. J. Quan. Info.* **2009**, *07* 125.
- [8] A. Fujiwara, H. Imai, *J. Phys. A: Math. Theor.* **2008**, *41* 255304.
- [9] B. M. Escher, R. L. de Matos Filho, L. Davidovich, *Nat. Phys.* **2011**, *7* 406–411.
- [10] X. Deng, S.-L. Chen, M. Zhang, X.-F. Xu, J. Liu, Z. Gao, X.-C. Duan, M.-K. Zhou, L. Cao, Z.-K. Hu, *Phys. Rev. A* **2021**, *104* 012607.
- [11] R. Demkowicz-Dobrzański, L. Maccone, *Phys. Rev. Lett.* **2014**, *113*, 25 250801.
- [12] R. Demkowicz-Dobrzański, J. Kołodyński, M. Guţă, *Nat. Commun.* **2012**, *3* 1063.
- [13] S. F. Huelga, C. Macchiavello, T. Pellizzari, A. K. Ekert, M. B. Plenio, J. I. Cirac, *Phys. Rev. Lett.* **1997**, *79* 3865.
- [14] A. W. Chin, S. F. Huelga, M. B. Plenio, *Phys. Rev. Lett.* **2012**, *109* 233601.
- [15] M. J. W. Hall, H. M. Wiseman, *Phys. Rev. X* **2012**, *2* 041006.
- [16] D. W. Berry, M. Tsang, M. J. Hall, H. M. Wiseman, *Phys. Rev. X* **2015**, *5* 031018.
- [17] S. Alipour, M. Mehboudi, A. T. Rezakhani, *Phys. Rev. Lett.* **2014**, *112* 120405.
- [18] M. Beau, A. del Campo, *Phys. Rev. Lett.* **2017**, *119* 010403.
- [19] R. Schnabel, N. Mavalvala, D. E. McClelland, P. K. Lam, *Nat. Commun.* **2010**, *1* 121.
- [20] Y.-S. Wang, C. Chen, J.-H. An, *New J. Phys.* **2017**, *19* 113019.
- [21] K. Bai, Z. Peng, H.-G. Luo, J.-H. An, *Phys. Rev. Lett.* **2019**, *123* 040402.
- [22] W. Wu, S.-Y. Bai, J.-H. An, *Phys. Rev. A* **2021**, *103* L010601.
- [23] J. Abadie, et al., *Nat. Phys.* **2011**, *7* 962.
- [24] T. Eberle, S. Steinlechner, J. Bauchrowitz, V. Händchen, H. Vahlbruch, M. Mehmet, H. Müller-Ebhardt, R. Schnabel, *Phys. Rev. Lett.* **2010**, *104* 251102.
- [25] S. Steinlechner, N.-O. Rohweder, M. Korobko, D. Töyrä, A. Freise, R. Schnabel, *Phys. Rev. Lett.* **2018**, *121* 263602.
- [26] H. Grote, K. Danzmann, K. L. Dooley, R. Schnabel, J. Slutsky, H. Vahlbruch, *Phys. Rev. Lett.* **2013**, *110* 181101.
- [27] M. Tse, et al., *Phys. Rev. Lett.* **2019**, *123* 231107.
- [28] J. Joo, W. J. Munro, T. P. Spiller, *Phys. Rev. Lett.* **2011**, *107* 083601.
- [29] B. L. Higgins, D. W. Berry, S. D. Bartlett, H. M. Wiseman, G. J. Pryde, *Nature* **2007**, *450* 393.
- [30] C. Schäfermeier, M. Ježek, L. S. Madsen, T. Gehring, U. L. Andersen, *Optica* **2018**, *5* 60.
- [31] C. Oh, C. Lee, C. Rockstuhl, H. Jeong, J. Kim, H. Nha, S.-Y. Lee, *npj Quantum Inf.* **2019**, *5* 10.
- [32] F. Wolfgramm, A. Cerè, F. A. Beduini, A. Predojević, M. Koschorreck, M. W. Mitchell, *Phys. Rev. Lett.* **2010**, *105* 053601.
- [33] B. B. Li, J. Bilek, U. B. Hoff, L. S. Madsen, S. Forstner, V. Prakash, C. Schäfermeier, T. Gehring, W. P. Bowen, U. L. Andersen, *Optica* **2018**, *5* 850.
- [34] R. C. Pooser, B. Lawrie, *Optica* **2015**, *2* 393.
- [35] Z. Huang, C. Lupo, P. Kok, *PRX Quantum* **2021**, *2* 030303.
- [36] Q. Zhuang, *Phys. Rev. Lett.* **2021**, *126* 240501.
- [37] Y. Michael, L. Bello, M. Rosenbluh, A. Pe’er, *npj Quantum Inf.* **2019**, *5* 81.
- [38] Y. Cai, J. Roslund, V. Thiel, C. Fabre, N. Treps, *npj Quantum Inf.* **2021**, *7* 82.
- [39] J. Liu, H. Yuan, X.-M. Lu, X. Wang, *J. Phys. A: Math. Theor.* **2020**, *53* 023001.
- [40] K. Li, Y. Cai, J. Wu, Y. Liu, S. Xiong, Y. Li, Y. Zhang, *Adv. Quantum Technol.* **2020**, *3* 1900119.
- [41] M. I. Kolobov, *Rev. Mod. Phys.* **1999**, *71* 1539.
- [42] L. A. Lugiato, A. Gatti, E. Brambilla, *J. Opt. B: Quantum Semiclass. Opt.* **2002**, *4* S176.
- [43] N. Treps, N. Grosse, W. P. Bowen, C. Fabre, H.-A. Bachor, P. K. Lam, *Science* **2003**, *301* 940.
- [44] P. A. Morris, R. S. Aspden, J. E. C. Bell, R. W. Boyd, M. J. Padgett, *Nat. Commun.* **2015**, *6* 5913.
- [45] W. Roga, J. Jeffers, *Phys. Rev. A* **2016**, *94* 032301.
- [46] M. Tsang, R. Nair, X.-M. Lu, *Phys. Rev. X* **2016**, *6* 031033.
- [47] C. A. Casacio, L. S. Madsen, A. Terrasson, M. Waleed, K. Barnscheidt, B. Hage, M. A. Taylor, W. P. Bowen, *Nature* **2021**, *594* 201–206.
- [48] J. H. Shapiro, S. Lloyd, *New J. Phys.* **2009**, *11* 063045.
- [49] E. D. Lopaeva, I. R. Berchera, I. P. Degiovanni, S. Olivares, G. Brida, M. Genovese, *Phys. Rev. Lett.* **2013**, *110*, 153603.
- [50] J. P. Dowling, *Phys. Rev. A* **1998**, *57* 4736.
- [51] Y. Che, J. Liu, X.-M. Lu, X. Wang, *Phys. Rev. A* **2019**, *99* 033807.
- [52] X. Guo, C. R. Breum, J. Borregaard, S. Izumi, M. V. Larsen, T. Gehring, M. Christandl, J. S. Neergaard-Nielsen, U. L. Andersen, *Nat. Phys.* **2020**, *16* 281.
- [53] Y. Xia, W. Li, W. Clark, D. Hart, Q. Zhuang, Z. Zhang, *Phys. Rev. Lett.* **2020**, *124* 150502.
- [54] S.-R. Zhao, Y.-Z. Zhang, W.-Z. Liu, J.-Y. Guan, W. Zhang, C.-L. Li, B. Bai, M.-H. Li, Y. Liu, L. You, J. Zhang, J. Fan, F. Xu, Q. Zhang, J.-W. Pan, *Phys. Rev. X* **2021**, *11* 031009.
- [55] J. J. Bollinger, W. M. Itano, D. J. Wineland, D. J. Heinzen, *Phys. Rev. A* **1996**, *54* R4649.
- [56] V. Bužek, R. Derka, S. Massar, *Phys. Rev. Lett.* **1999**, *82* 2207.
- [57] D. Leibfried, M. D. Barrett, T. Schaetz, J. Britton, J. Chiaverini, W. M. Itano, J. D. Jost, C. Langer, D. J. Wineland, *Science* **2004**, *304* 1476.
- [58] C. F. Roos, M. Chwalla, K. Kim, M. Riebe, R. Blatt, *Nature* **2006**, *443* 316.

- [59] A. Derevianko, H. Katori, *Rev. Mod. Phys.* **2011**, 83 331.
- [60] A. D. Ludlow, M. M. Boyd, J. Ye, E. Peik, P. O. Schmidt, *Rev. Mod. Phys.* **2015**, 87 637.
- [61] J. Borregaard, A. S. Sørensen, *Phys. Rev. Lett.* **2013**, 111 090801.
- [62] M. A. Taylor, J. Janousek, V. Daria, J. Knittel, B. Hage, H.-A. Bachor, W. P. Bowen, *Nat. Photon.* **2013**, 7 229.
- [63] M. Hayashi, *Phys. Lett. A* **2006**, 354 183.
- [64] H. Imai, M. Hayashi, *New J. Phys.* **2009**, 11 043034.
- [65] M. Hayashi, *Commun. Math. Phys.* **2011**, 304 689–709.
- [66] S. Massar, S. Popescu, *Phys. Rev. Lett.* **1995**, 74 1259.
- [67] A. S. Holevo, *IEEE Trans. Inf. Theory* **1998**, 44 269.
- [68] G. Chiribella, G. M. D'Ariano, P. Perinotti, M. F. Sacchi, *Phys. Rev. A* **2004**, 70 062105.
- [69] G. Chiribella, G. M. D'Ariano, M. F. Sacchi, *Phys. Rev. A* **2005**, 72 042338.
- [70] A. Bisio, G. Chiribella, G. M. D'Ariano, S. Facchini, P. Perinotti, *Phys. Rev. A* **2010**, 81 032324.
- [71] R. Demkowicz-Dobrzański, W. Górecki, M. Guță, *J. Phys. A: Math. Theor.* **2020**, 53 363001.
- [72] F. Albarelli, M. Barbieri, M. G. Genoni, I. Gianani, *Phys. Lett. A* **2020**, 384 126311.
- [73] J. S. Sidhu, P. Kok, *AVS Quantum Sci.* **2020**, 2 014701.
- [74] H. Cramer, *Mathematical Methods of Statistics*, Princeton University, **1946**.
- [75] C. R. Rao, *Bull. Calcutta Math. Soc.* **1945**, 37 81.
- [76] R. A. Fisher, *Proc. Camb. Phil. Soc.* **1925**, 22 700.
- [77] W. K. Wootters, *Phys. Rev. D* **1981**, 23 357.
- [78] M. A. Nielsen, I. Chuang, *Quantum computation and quantum information*, **2002**.
- [79] J. Liu, H.-N. Xiong, F. Song, X. Wang, *Physica A: Statistical Mechanics and its Applications* **2014**, 410 167.
- [80] H. Yuan, C.-H. F. Fung, *New J. Phys.* **2017**, 19 113039.
- [81] A. Uhlmann, *Rep. Math. Phys.* **1976**, 9 273.
- [82] V. P. Belavkina, G. M. D'Ariano, M. Raginsky, *J. Math. Phys.* **2005**, 46 062106.
- [83] H. Yuan, C.-H. F. Fung, *npj Quantum Inf.* **2017**, 3 14.
- [84] A. Bhattacharyya, *Bull. Calcutta Math. Soc.* **1943**, 35 99.
- [85] M. Sarovar, G. J. Milburn, *J. Phys. A: Math. Gen.* **2006**, 39 8487.
- [86] J. Kołodyński, R. Demkowicz-Dobrzański, *New J. Phys.* **2013**, 15 073043.
- [87] H. Yuan, C.-H. F. Fung, *Phys. Rev. A* **2017**, 96 012310.
- [88] C. M. Caves, *Phys. Rev. D* **1981**, 23 1693.
- [89] J. Liu, X.-X. Jing, X. Wang, *Phys. Rev. A* **2013**, 88 042316.
- [90] X. Yu, X. Zhao, L. Shen, Y. Shao, J. Liu, X. Wang, *Opt. Express* **2018**, 26 16292.
- [91] H. Liang, J. Pei, X. Wang, *Chin. Phys. Lett.* **2020**, 37 070301.
- [92] M. Jarzyna, R. Demkowicz-Dobrzański, *Phys. Rev. A* **2012**, 85 011801(R).
- [93] M. D. Lang, C. M. Caves, *Phys. Rev. Lett.* **2013**, 111 173601.
- [94] M. D. Lang, C. M. Caves, *Phys. Rev. A* **2014**, 90 025802.
- [95] D. W. Berry, H. M. Wiseman, *Phys. Rev. Lett.* **2000**, 85 5098.
- [96] D. W. Berry, H. M. Wiseman, J. K. Breslin, *Phys. Rev. A* **2001**, 63 053804.
- [97] B. C. Sanders, G. J. Milburn, *Phys. Rev. Lett.* **1995**, 75 2944.
- [98] A. S. Holevo, *Springer Lecture Notes Math.* **1984**, 1055 153.
- [99] A. Fujiwara, *Phys. Rev. A* **2001**, 63 042304.
- [100] G. Tóth, I. Apellaniz, *J. Phys. A: Math. Theor.* **2014**, 47 424006.
- [101] M. Takeoka, K. P. Seshadreesan, C. You, S. Izumi, J. P. Dowling, *Phys. Rev. A* **2017**, 96 052118.
- [102] K. Modi, H. Cable, M. Williamson, V. Vedral, *Phys. Rev. X* **2011**, 1 021022.
- [103] L. J. Fiderer, J. M. E. Fraïsse, D. Braun, *Phys. Rev. Lett.* **2019**, 123 250502.
- [104] L. A. Correa, M. Mehboudi, G. Adesso, A. Sanpera, *Phys. Rev. Lett.* **2015**, 114 220405.
- [105] A. Monras, *Phys. Rev. A* **2006**, 73 033821.
- [106] D. Šafránek, I. Fuentes, *Phys. Rev. A* **2016**, 94 062313.
- [107] S. Knysh, E. H. Chen, G. A. Durkin, *arXiv*: 1402.0495, **2014**.
- [108] U. Dorner, R. Demkowicz-Dobrzański, B. J. Smith, J. S. Lundeen, W. Wasilewski, K. Banaszek, I. A. Walmsley, *Phys. Rev. Lett.* **2009**, 102 040403.
- [109] R. Demkowicz-Dobrzański, U. Dorner, B. J. Smith, J. S. Lundeen, W. Wasilewski, K. Banaszek, I. A. Walmsley, *Phys. Rev. A* **2009**, 80 013825.
- [110] A. Forsgren, P. E. Gill, M. H. Wright, *SIAM Rev.* **2002**, 44 525–597.
- [111] L. Maccone, G. De Cillis, *Phys. Rev. A* **2009**, 79 023812.
- [112] S. Knysh, V. N. Smelyanskiy, G. A. Durkin, *Phys. Rev. A* **2011**, 83 021804.
- [113] F. Fröwis, M. Skotiniotis, B. Kraus, W. Dür, *New J. Phys.* **2014**, 16 083010.
- [114] J. A. Nelder, R. Mead, *Comput. J.* **1965**, 7 308–313.
- [115] S. Zhou, L. Jiang, *Phys. Rev. Research* **2020**, 2 013235.
- [116] P. A. Knott, *New J. Phys.* **2016**, 18 073033.
- [117] J. Kennedy, R. Eberhar, *Proc. 1995 IEEE International Conference on Neural Networks* **1995**, 4 1942.
- [118] R. S. Sutton, D. A. McAllester, S. P. Singh, Y. Mansour, *Proc. 1995 IEEE International Conference on Neural Networks* **1999**, 1057–1063.
- [119] T. P. Lillicrap, J. J. Hunt, A. Pritzel, N. Heess, T. Erez, Y. Tassa, D. Silver, D. Wierstra, *arXiv*: 1509.02971, **2015**.
- [120] J. Liu, H. Yuan, *Phys. Rev. A* **2017**, 96 012117.
- [121] V. Mnih, A. P. Badia, M. Mirza, A. Graves, T. P. Lillicrap, T. Harley, D. Silver, K. Kavukcuoglu, *arXiv*: 1602.01783, **2016**.
- [122] H. Yuan, C.-H. F. Fung, *Phys. Rev. Lett.* **2015**, 115 110401.
- [123] H. Yuan, *Phys. Rev. Lett.* **2016**, 117 160801.
- [124] Z. Hou, R.-J. Wang, J.-F. Tang, H. Yuan, G.-Y. Xiang, C.-F. Li, G.-C. Guo, *Phys. Rev. Lett.* **2019**, 123 040501.
- [125] Z. Hou, J.-F. Tang, H. Chen, H. Yuan, G.-Y. Xiang, C.-F. Li, G.-C. Guo, *Sci. Adv.* **2021**, 7 eabd2986.
- [126] S. Pang, A. N. Jordan, *Nat. Commun.* **2017**, 8 14695.
- [127] Q.-S. Tan, M. Zhang, Y. Chen, J.-Q. Liao, J. Liu, *Phys. Rev. A* **2021**, 103 032601.
- [128] N. Khaneja, T. Reiss, C. Hehlet, T. Schulte-Herbruggen, S. J. Glaser, *J. Magn. Reson.* **2005**, 172 296.
- [129] J. Liu, H. Yuan, *Phys. Rev. A* **2017**, 96 042114.
- [130] D. Basilewitsch, H. Yuan, C. P. Koch, *Phys. Rev. Research* **2020**, 2 033396.
- [131] J. Li, X. Yang, X. Peng, C.-P. Sun, *Phys. Rev. Lett.* **2017**, 118 150503.

- [132] X. Yang, J. Thompson, Z. Wu, M. Gu, X. Peng, J. Du, *npj Quantum Inf.* **2020**, 6 62.
- [133] X. Yang, X. Chen, J. Li, X. Peng, R. Lafamme, *Sci. Rep.* **2021**, 11 672.
- [134] R.-B. Wu, B. Chu, D. H. Owens, H. Rabitz, *Phys. Rev. A* **2018**, 97 042122.
- [135] R.-B. Wu, H. Ding, D. Dong, X. Wang, *Phys. Rev. A* **2019**, 99 042327.
- [136] H.-J. Ding, R.-B. Wu, *Phys. Rev. A* **2019**, 100 022302.
- [137] X. Ge, H. Ding, H. Rabitz, R.-B. Wu, *Phys. Rev. A* **2020**, 101 052317.
- [138] H. Xu, J. Li, L. Liu, Y. Wang, H. Yuan, X. Wang, *npj Quantum Inf.* **2019**, 5 82.
- [139] H. Xu, L. Wang, H. Yuan, X. Wang, *Phys. Rev. A* **2021**, 103 042615.
- [140] Q. Zheng, L. Ge, Y. Yao, Q. Zhi, *Phys. Rev. A* **2015**, 91 033805.
- [141] L. Liu, H. Yuan, *Phys. Rev. A* **2020**, 102 012208.
- [142] Y. Yang, *Phys. Rev. Lett.* **2019**, 123 110501.
- [143] A. Altherr, Y. Yang, *Phys. Rev. Lett.* **2021**, 127 060501.
- [144] P. W. Shor, *Phys. Rev. A* **1995**, 52 R2493.
- [145] A. M. Steane, *Phys. Rev. Lett.* **1996**, 77 793.
- [146] E. Knill, R. Laflamme, *Phys. Rev. A* **1997**, 55 900.
- [147] D. Gottesman, *Proc. Symp. Appl. Math.* **2010**, 68 13.
- [148] D. G. Cory, M. D. Price, W. Maas, E. Knill, R. Laflamme, W. H. Zurek, T. F. Havel, S. S. Somaroo, *Phys. Rev. Lett.* **1998**, 81 2152.
- [149] J. Chiaverini, D. Leibfried, T. Schaetz, M. D. Barrett, R. B. Blakestad, J. Britton, W. M. Itano, J. D. Jost, E. Knill, C. Langer, R. Ozeri, D. J. Wineland, *Nature* **2004**, 432 602.
- [150] E. Knill, R. Laflamme, *arXiv: quant-ph/9608012*, **1996**.
- [151] J. Preskill, *arXiv: quant-ph/9712048*, **1997**.
- [152] D. Aharonov, M. Ben-Or, *arXiv: quant-ph/9906129*, **1999**.
- [153] C. Chamberland, T. Jochym-O'Connor, R. Laflamme, *Phys. Rev. Lett.* **2016**, 117 010501.
- [154] B. Schumacher, M. D. Westmoreland, *Phys. Rev. A* **1997**, 56 131.
- [155] M. M. Wilde, *Quantum Information Theory*, Cambridge University Press, **2013**.
- [156] E. M. Kessler, I. Lovchinsky, A. O. Sushkov, M. D. Lukin, *Phys. Rev. Lett.* **2014**, 112 150802.
- [157] G. Arrad, Y. Vinkler, D. Aharonov, A. Retzker, *Phys. Rev. Lett.* **2014**, 112 150801.
- [158] W. Dür, M. Skotiniotis, F. Froewis, B. Kraus, *Phys. Rev. Lett.* **2014**, 112 080801.
- [159] X.-M. Lu, S. Yu, C. H. Oh, *Nat. Commun.* **2015**, 6 7282.
- [160] Y. Matsuzaki, S. Benjamin, *Phys. Rev. A* **2017**, 95 032303.
- [161] P. Sekatski, M. Skotiniotis, J. Kołodyński, W. Dür, *Quantum* **2017**, 1 27.
- [162] R. Demkowicz-Dobrzański, J. Czajkowski, P. Sekatski, *Phys. Rev. X* **2017**, 7 041009.
- [163] D. Layden, S. Zhou, P. Cappellaro, L. Jiang, *Phys. Rev. Lett.* **2019**, 122 040502.
- [164] Y. Chen, H. Chen, J. Liu, Z. Miao, H. Yuan, *arXiv: 2003.13010*, **2020**.
- [165] W. Górecki, S. Zhou, L. Jiang, R. Demkowicz-Dobrzański, *Quantum* **2020**, 4 288.
- [166] S. Zhou, M. Zhang, J. Preskill, L. Jiang, *Nat. Commun.* **2018**, 9 78.
- [167] A. Hentschel, B. C. Sanders, *Phys. Rev. Lett.* **2010**, 104 063603.
- [168] R. Eberhart, J. Kennedy, *Proceedings of the Sixth International Symposium on Micro Machine and Human Science*, New York: IEEE, **1995**.
- [169] A. Hentschel, B. C. Sanders, *Phys. Rev. Lett.* **2011**, 107 233601.
- [170] P. Palittapongarnpim, P. Wittek, E. Zahedinejad, S. Vedaie, B. C. Sanders, *Neurocomputing* **2017**, 268 116.
- [171] P. Palittapongarnpim, B. C. Sanders, *Phys. Rev. A* **2019**, 100 012106.
- [172] Y. Peng, H. Fan, *Phys. Rev. A* **2020**, 101 022107.
- [173] A. Lumino, E. Polino, A. S. Rab, G. Milani, N. Spagnolo, N. Wiebe, F. Sciarrino, *Phys. Rev. Applied* **2018**, 10 044033.
- [174] K. Rambhatla, S. E. D'Aurelio, M. Valeri, E. Polino, N. Spagnolo, F. Sciarrino, *Phys. Rev. Research* **2020**, 2 033078.
- [175] N. B. Lovett, C. Crosnier, M. Perarnau-Llobet, B. C. Sanders, *Phys. Rev. Lett.* **2013**, 110 220501.
- [176] H. M. Wiseman, *Phys. Rev. Lett.* **1995**, 75 4587.
- [177] H. M. Wiseman, R. B. Killip, *Phys. Rev. A* **1997**, 56 944.
- [178] H. M. Wiseman, R. B. Killip, *Phys. Rev. A* **1998**, 57 2169.
- [179] M. A. Armen, J. K. Au, J. K. Stockton, A. C. Doherty, H. Mabuchi, *Phys. Rev. Lett.* **2002**, 89 133602.
- [180] G. M. D'Ariano, M. G. A. Paris, R. Seno, *Phys. Rev. A* **1996**, 54 4495.
- [181] S. Olivares, M. G. A. Paris, *J. Phys. B: At. Mol. Opt. Phys.* **2009**, 42 055506.
- [182] S. Gammelmark, K. Mølmer, *Phys. Rev. A* **2013**, 87 032115.
- [183] S. Gammelmark, K. Mølmer, *Phys. Rev. Lett.* **2014**, 112 170401.
- [184] A. H. Küllerich, K. Mølmer, *Phys. Rev. A* **2016**, 94 032103.
- [185] F. Albarelli, M. A. C. Rossi, D. Tamascelli, M. G. Genoni, *Quantum* **2018**, 2 110.
- [186] M. A. C. Rossi, F. Albarelli, D. Tamascelli, M. G. Genoni, *Phys. Rev. Lett.* **2020**, 125 200505.
- [187] F. Albarelli, M. A. C. Rossi, M. G. A. Paris, M. G. Genoni, *New J. Phys.* **2017**, 19 123011.
- [188] A. A. Berni, T. Gehring, B. M. Nielsen, V. Händchen, M. G. A. Paris, U. L. Andersen, *Nat. Photon.* **2015**, 9 577–581.
- [189] T. A. Wheatley, D. W. Berry, H. Yonezawa, D. Nakane, H. Arao, D. T. Pope, T. C. Ralph, H. M. Wiseman, A. Furusawa, E. H. Huntington, *Phys. Rev. Lett.* **2010**, 104 093601.
- [190] M. Tsang, *Phys. Rev. Lett.* **2009**, 102 250403.
- [191] N. Wiebe, C. Granade, *Phys. Rev. Lett.* **2016**, 117 010503.
- [192] K. Zheng, H. Xu, A. Zhang, X. Ning, L. Zhang, *Quantum Inf. Process.* **2019**, 18 329.
- [193] M. Valeri, E. Polino, D. Poderini, I. Gianani, G. Corrielli, A. Crespi, R. Osellame, N. Spagnolo, F. Sciarrino, *npj Quantum Inf.* **2020**, 6 92.
- [194] L. J. Fiderer, J. Schuff, D. Braun, *PRX Quantum* **2021**, 2 020303.
- [195] S. Steinlechner, J. Bauchrowitz, M. Meinders, H. Müller-Ebhardt, K. Danzmann, R. Schnabel, *Nat. Photon.* **2013**, 7 626.



- [196] M. Tsang, F. Albarelli, A. Datta, *Phys. Rev. X* **2020**, *10* 031023.
- [197] J. Suzuki, Y. Yang, M. Hayashi, *J. Phys. A: Math. Theor.* **2020**, *53* 453001.
- [198] M. Szczykulska, T. Baumgratz, A. Datta, *Adv. Phys. X* **2016**, *1* 621.
- [199] J. Rubio, J. Dunningham, *New J. Phys.* **2019**, *21* 043037.
- [200] M. Tsang, *Phys. Rev. Lett.* **2012**, *108* 230401.
- [201] X.-M. Lu, M. Tsang, *Quantum Sci. Technol.* **2016**, *1* 015002.
- [202] J. Liu, H. Yuan, *New J. Phys.* **2016**, *18* 093009.